Chiral Recognition in Molecular and Macromolecular Pairs of Liquid Crystals of (2*R*,3*S*)- and (2*S*,3*S*)-2-Fluoro-3-methylpentyl 4′-[[11-(Vinyloxy)undecanyl]oxy]biphenyl-4-carboxylate Diastereomers

V. Percec* and H. Oda

Department of Macromolecular Science, Case Western Reserve University, Cleveland, Ohio 44106

P. L. Rinaldi and D. R. Hensley

Department of Chemistry, University of Akron, Akron, Ohio 44325

Received May 25, 1993; Revised Manuscript Received October 13, 1993®

ABSTRACT: (2*R*,3*S*)-2-Fluoro-3-methylpentyl 4′-[[11-(vinyloxy)undecanyl]oxy]biphenyl-4-carboxylate (**15**; 2*R*, 92% ee) and (2*S*,3*S*)-2-fluoro-3-methylpentyl 4′-[[11-(vinyloxy)undecanyl]oxy]biphenyl-4-carboxylate (**16**; 2*S*, 96% ee) diastereomers and their corresponding homopolymers and copolymers with well-defined molecular weights and narrow molecular weight distributions were synthesized and characterized. The phase behavior of the two diastereomeric polymers can be compared only by superimposing the dependence of their transition temperatures as a function of molecular weight. The phase behaviors of **15** and poly(**15**) are identical to those of **16** and poly(**16**), respectively, except that the monomers show slightly different transition temperatures and enthalpy changes from each other. Both monomers display enantiotropic S_A, monotropic S_C*, and S_X (unidentified smectic) phases and a crystalline phase, while the corresponding polymers exhibit enantiotropic S_A, S_C*, and S_X mesophases. Phase diagrams were investigated in detail in binary mixtures of **15** with **16** and poly(**15**) with poly(**16**) and in binary copolymers of **15** with **16** as a function of the composition of the two diastereomeric structural units. In all these systems the two diastereomeric structural units derived from the two monomers are miscible and therefore isomorphic within all their mesophases and over the entire range of compositions. This is in contrast to the crystalline phases of the monomers whose phase diagram displays an eutectic composition. The S_A–I transition of the binary mixture of **15** with **16** is with 0.2–0.4 °C higher in the 50/50 mixture than the theoretical value expected for an ideal solution, demonstrating the presence of chiral molecular recognition between the two diastereomers in their S_A phase. In the polymer and copolymer systems chiral molecular recognition present in the monomers seems to be canceled or it is too small to be detected. On the contrary, the S_A–S_C* and S_C*–S_X transition temperatures show negative deviations from the theoretical ideal values in all systems, indicating the nonideal solution behavior of the two diastereomeric structural units in the S_C* and S_X phases.

Introduction

Stereochemistry is the most sensitive tool for probing the structural details on how molecules "see" each other as they come together to form ordered structures and transition states. Therefore, it represents the most powerful tool available in chemistry for the study and manipulation of molecular shapes and symmetry properties.[1] The most notable series of studies in this field refers to the investigation of chiral molecular recognition in monolayers of pure enantiomers and their pairs as well as in monolayers of pure diastereomers and their mixtures.[1a,b] Enantiomers are considered to be perfect physical and chemical models for each other since their properties, with the exception of the rotation of polarized light and those that involve their interactions with other chiral systems, are identical. Chiral discrimination between the properties of monolayers formed by pure enantiomers and their mixtures was always observed,[1,2] with the notable exception of phosphatidylcholines.[3]

In the field of molecular thermotropic liquid crystals, there are a significant number of examples in which the phase behavior of binary mixtures of enantiomeric compounds was compared to that of the pure enantiomers.[1c,d,4-7] In these examples it has been observed that chiral molecular recognition occurs and it increases the phase transition temperatures of the 1/1 molar mixture in comparison to the one of the pure enantiomers.

There are much fewer systems in which attempts were made to detect stereochemical recognition between pairs of diastereomers in monolayers. The first systematic study of the monolayer properties of a diastereomeric series was reported in 1988.[8a] By contrast to pairs of enantiomers[1a,b,2] none of the first eight pairs of diastereomeric surfactants investigated showed stereoselectivity at the air–water interface.[8a] Only very recently was the first example of chiral molecular recognition in monolayers of diastereomeric compounds reported.[8b]

The first goal of this paper is to describe the synthesis and the living cationic polymerization of (2*R*,3*S*)-2-fluoro-3-methylpentyl 4′-[[11-(vinyloxy)undecanyl]oxy]biphenyl-4-carboxylate (**15**) and (2*S*,3*S*)-2-fluoro-3-methylpentyl 4′-[[11-(vinyloxy)undecanyl]oxy]biphenyl-4-carboxylate (**16**) diastereomers. The second goal of this paper is to compare the mesomorphic behavior of these two diastereomeric structural units and to investigate their chiral recognition in binary monomer and polymer mixtures, and in binary copolymers. To our knowledge, this paper reports the first investigation on the chiral molecular recognition of molecular and macromolecular pairs of diastereomeric liquid crystals.

Experimental Section

Materials. L-Isoleucine [(2*S*,3*S*)-(+)-2-amino-3-methylpentanoic acid, 99%], tetrabutylammonium fluoride hydrate (*n*-

* To whom all correspondence should be addressed.

® Abstract published in *Advance ACS Abstracts*, December 1, 1993.

0024-9297/94/2227-0012$04.50/0

$Bu_4NF{\cdot}xH_2O$, 98%), tetrabutylammonium hydrogen sulfate (TBAH, 98%), and pyridinium poly(hydrogen fluoride) (HF, 70% by weight) (all from Aldrich) were used as received.

$NaNO_2$ (Fisher) was dried at 140 °C under vacuum for 40 h before each use. Trifluoromethanesulfonic anhydride was prepared from CF_3SO_3H (Lancaster; 98+%) and P_2O_5 according to a literature procedure.[9a,b]

Pyridine was heated overnight at 100 °C over KOH, distilled from KOH, and then stored over KOH. CH_2Cl_2 was refluxed over CaH_2 overnight and distilled from CaH_2. Dimethyl sulfoxide (DMSO) was heated overnight at 100 °C over CaH_2, distilled from CaH_2 under vacuum, and stored over molecular sieves (4 Å). Tetrahydrofuran (THF) was first distilled from $LiAlH_4$ and further dried over sodium benzophenone.

CH_2Cl_2 used as the polymerization solvent was first washed with concentrated H_2SO_4 several times until the acid layer remained colorless, then washed with water, dried over $MgSO_4$, refluxed over CaH_2, and freshly distilled under argon before each use. $(CH_3)_2S$ used in polymerizations (Aldrich; anhydrous, 99+%, packed under nitrogen in a Sure/Seal bottle) was used as received. CF_3SO_3H used as a polymerization initiator (Aldrich; 98%) was distilled under vacuum.

All other materials were commercially available and were used as received.

Techniques. ^{1}H-NMR (200-MHz) spectra were recorded on a Varian XL-200 spectrometer. ^{19}F-decoupled ^{1}H-NMR (300-MHz) spectra and ^{19}F-NMR spectra were recorded on a Varian VXR-300 spectrometer. In order to determine the chemical shifts of ^{19}F resonances, a ^{19}F spectrum of $CF_3C_6H_5$ was first acquired since its ^{19}F resonance is known from the literature[10] to appear at 63.72 ppm (referenced against $CFCl_3$ at 0.00 ppm). Then sample spectra were acquired using the identical parameters.

Relative molecular weights of polymers were determined by gel permeation chromatography (GPC). GPC analyses were carried out with a Perkin-Elmer Series 10LC instrument equipped with an LC-100 column oven and a Nelson Analytical 900 Series datastation. Measurements were made by using a UV detector, THF as solvent (1 mL/min, 40 °C), a set of PL gel columns of 5×10^2 and 10^4 Å, and a calibration plot constructed with polystyrene standards. High-pressure liquid chromatography (HPLC) experiments were performed with the same instrument.

Two types of differential scanning calorimetry were used to determine the thermal transition temperatures. A Perkin-Elmer DSC-4 equipped with a TADS 3600 datastation was used to analyze the homopolymers and the copolymers. Heating and cooling rates were 20 °C/min. A Perkin-Elmer PC Series DSC-7 was used to analyze the monomer mixtures and the polymer mixtures. Heating and cooling rates were 10 °C/min. In all cases the thermal transition temperatures were reported as the maxima and minima of their endothermic or exothermic peaks, respectively.

X-ray diffraction measurements were performed with a Rigaku powder diffractometer. A monochromatized X-ray beam from Cu Kα radiation with a wavelength of 0.154 18 nm was used. A temperature controller was added to the X-ray apparatus for thermal measurements. The precision of the controller was ±0.5 °C in the temperature range studied.

A Carl–Zeiss optical polarizing microscope equipped with a Mettler FP-82 hot stage and a Mettler FP-80 central processor was used to observe the thermal transitions and to analyze the anisotropic textures.

Synthesis of Monomers. Monomers 15 and 16 were synthesized according to Scheme 1. The synthesis of compounds 11 and 14 was described previously.[11]

(2*S*,3*S*)-2-Hydroxy-3-methylpentanoic Acid (2).[12] A solution of $NaNO_2$ (39.4 g, 0.572 mol) in water (150 mL) was added dropwise to a stirred, cooled (0 °C) mixture of L-isoleucine (49.5 g, 0.377 mol), concentrated H_2SO_4 (16 mL), and water (570 mL). The mixture was allowed to warm to room temperature and stirred overnight. The product was extracted into diethyl ether three times, and the combined ethereal extracts were dried over anhydrous $MgSO_4$. The crude product (39.5 g) obtained after the evaporation of the solvent was used for the synthesis of 3 without further purification. ^{1}H-NMR (DMSO-d_6, TMS): δ 0.84 (t, J = 7.2 Hz, 3H, CH_3CH_2–), 0.87 (d, J = 6.4 Hz, 3H, –CH(CH_3)–), 1.02–1.29, 1.29–1.53 (m, 2H, CH_3CH_2–), 1.53–1.57 (m, 1H, –CH(CH_3)–), 3.79 (d, J = 4.8 Hz, 1H, –CH(OH)–).

Scheme 1. Synthesis of Monomers 15 and 16

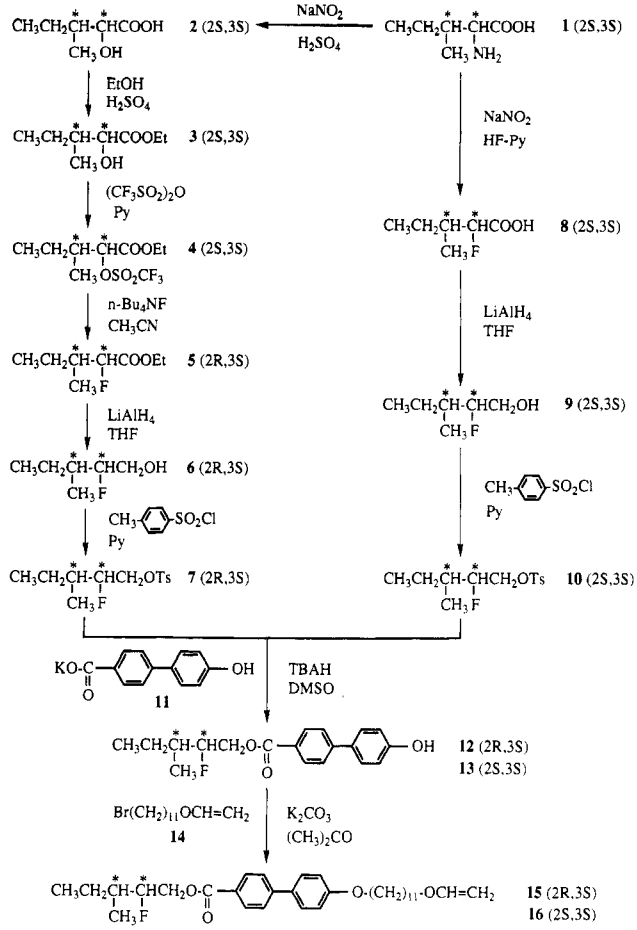

Ethyl (2*S*,3*S*)-2-Hydroxy-3-methylpentanoate (3).[12a] A stirred mixture of 2 (crude, 39.5 g), anhydrous ethanol (300 mL), and concentrated H_2SO_4 (7.5 mL) was heated under reflux overnight. Ethanol was distilled off, and the residue was diluted with diethyl ether. This ether solution was washed with saturated $NaHCO_3$ solution twice and dried over anhydrous $MgSO_4$. Ether was evaporated off, and the remaining crude product was distilled under vacuum to yield a colorless liquid (34.5 g, 57.1% from L-isoleucine). Bp: 62–65 °C (6 mmHg). ^{1}H-NMR ($CDCl_3$, TMS): δ 0.91 (t, J = 7.4 Hz, 3H, $CH_3CH_2CH(CH_3)$–), 0.99 (d, J = 6.7 Hz, 3H, –CH(CH_3)–), 1.13–1.53 (m, 2H, CH_3CH_2CH-(CH_3)–), 1.31 (t, J = 7.1 Hz, –$COOCH_2CH_3$), 1.73–1.93 (m, 1H, –CH(CH_3)–), 2.78 (b s, 1H, –CH(OH)–), 4.08 (d, J = 3.6 Hz, 1H, –CH(OH)–), 4.26 (dq, J = 7.1 and 1.7 Hz, 2H, –$COOCH_2CH_3$).

Ethyl (2*S*,3*S*)-2-[[(Trifluoromethyl)sulfonyl)oxy]-3-methylpentanoate (4).[9,12a] Freshly prepared trifluoromethanesulfonic anhydride (50.0 g, 0.177 mol) was added dropwise to a stirred, cooled (0 °C) solution of 3 (23.8 g, 0.149 mol) in dry CH_2Cl_2 (200 mL) and pyridine (18.6 mL, 0.230 mol) under a nitrogen atmosphere. The mixture was allowed to warm to room temperature and stirred for 2 h. Then the mixture was poured into water, and the product was extracted into CH_2Cl_2 twice. The combined organic layers were washed with 10% HCl twice and dried over anhydrous $MgSO_4$. The solvent was evaporated off, and the remaining crude product was distilled under vacuum to yield a colorless liquid (37.2 g, 85.4%). Bp: 55–61 °C (0.4 mmHg). ^{1}H-NMR ($CDCl_3$, TMS): δ 0.95 (t, J = 7.4 Hz, 3H, $CH_3CH_2CH(CH_3)$–), 1.07 (d, J = 7.0 Hz, 3H, –CH(CH_3)–), 1.19–1.64 (m, 2H, $CH_3CH_2CH(CH_3)$–), 1.33 (t, J = 7.2 Hz, 3H, –$COOCH_2CH_3$), 2.05–2.27 (m, 1H, –CH(CH_3)–), 4.31 (dq, J = 7.2 and 1.9 Hz, 2H, –$COOCH_2CH_3$), 5.01 (d, J = 3.9 Hz, 1H, –CH(OSO_2CF_3)–).

Ethyl (2*R*,3*S*)-2-Fluoro-3-methylpentanoate (5).[12a] A solution of 4 (36.7 g, 0.126 mol) in acetonitrile (50 mL) was added dropwise to a stirred, cooled (0 °C) solution of tetrabutylammonium fluoride hydrate (n-$Bu_4NF{\cdot}xH_2O$, 40 g) in acetonitrile

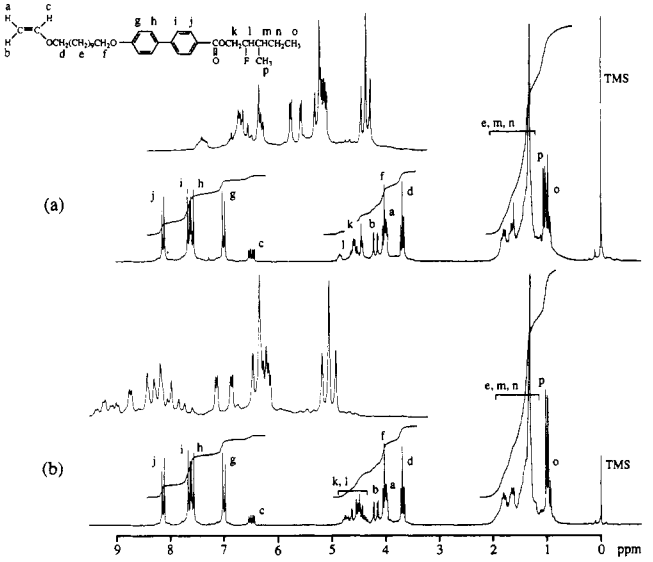

Figure 1. ^{1}H-NMR spectra of monomers (a) **15** and (b) **16**.

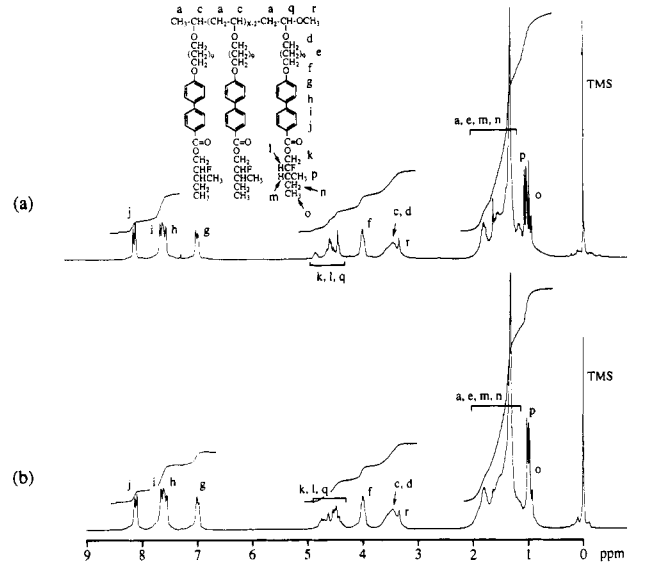

Figure 2. ^{1}H-NMR spectra of polymers (a) poly(**15**) (DP = 6.0) and (b) poly(**16**) (DP = 5.5).

(150 mL). The stirred mixture was heated under reflux for 3 h. Then acetonitrile was evaporated off, and the remaining mixture was passed through a silica gel short column using hexane–ethyl acetate (10:1) as an eluent. The solvent was evaporated off, and the crude product was distilled under vacuum to yield a colorless liquid (16.7 g, 81.9%). Bp: 59–63 °C (9 mmHg). ^{1}H-NMR ($CDCl_3$, TMS): δ 0.95 (d, J = 6.5 Hz, 3H, $-CH(CH_3)-$), 0.96 (t, J = 8.3 Hz, 3H, $CH_3CH_2CH(CH_3)-$), 1.19–1.65 (m, 2H, $CH_3CH_2-CH(CH_3)-$), 1.32 (t, J = 7.0 Hz, 3H, $-COOCH_2CH_3$), 1.75–2.12 (m, 1H, $-CH(CH_3)-$), 4.28 (q, J = 7.0 Hz, 2H, $-COOCH_2CH_3$), 4.86 (dd, J = 48.5 and 3.1 Hz, 1H, $-CHF-$).

(2*R*,3*S*)-2-Fluoro-3-methylpentanol (6).[12a] A solution of **5** (16.4 g, 0.101 mol) in dry THF (100 mL) was added dropwise to a stirred, cooled (−70 °C) mixture of $LiAlH_4$ (5.69 g, 0.150 mol) and dry THF (100 mL) under a nitrogen atmosphere. The stirred mixture was allowed to warm to room temperature and then heated under reflux for 2 h. Excess $LiAlH_4$ was quenched with ethyl acetate (50 mL), and the mixture was treated with 10% HCl (300 mL). The product was extracted into ethyl acetate twice, and the combined organic layers were dried over anhydrous $MgSO_4$. The solvent was evaporated off, and the remaining crude product was purified by column chromatography (silica gel; hexane–ethyl acetate 10:1 and 5:1) to give a colorless liquid (8.51 g, 70.1%). ^{1}H-NMR ($CDCl_3$, TMS); δ 0.93 (t, J = 7.6 Hz, 3H, CH_3CH_2-), 0.95 (d, J = 7.0 Hz, 3H, $-CH(CH_3)-$), 1.08–1.29, 1.36–1.76 (m, 3H, $CH_3CH_2CH(CH_3)-$), 2.81 (b s, 1H, $-OH$), 3.56–3.92 (m, 2H, $-CH_2OH$), 4.25–4.39, 4.50–4.62 (m, 1H, $-CHF-$).

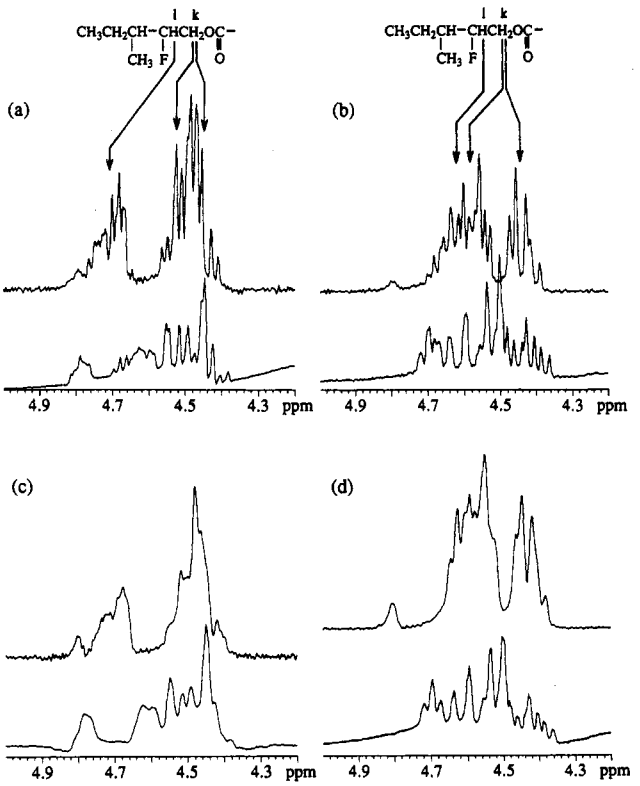

Figure 3. ^{19}F-decoupled ^{1}H-NMR spectra (top) and normal ^{1}H-NMR spectra (bottom) of monomers and polymers: (a) **15**; (b) **16**; (c) poly(**15**) (DP = 6.0); (d) poly(**16**) (DP = 5.5).

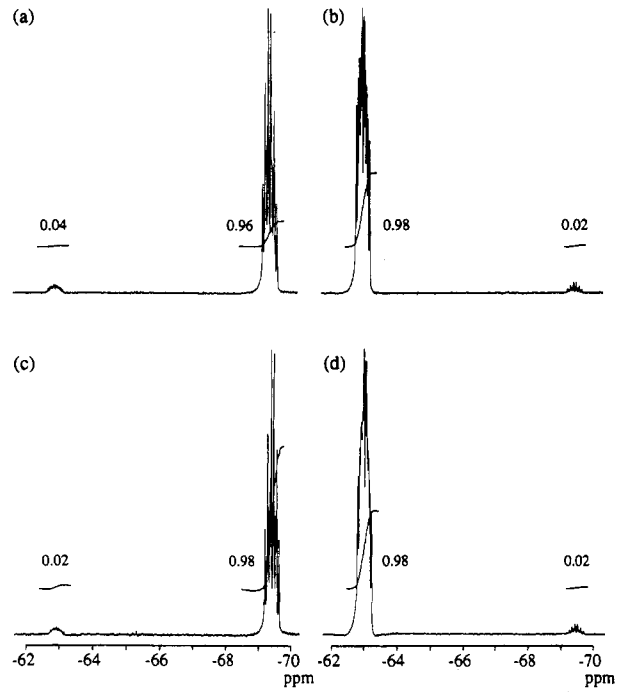

Figure 4. ^{19}F-NMR spectra of monomers and polymers: (a) **15**; (b) **16**; (c) poly(**15**) (DP = 6.0); (d) poly(**16**) (DP = 5.5).

(2*R*,3*S*)-2-Fluoro-3-methylpentyl Tosylate (7). A solution of **6** (4.0 g, 33.3 mmol) in dry pyridine (15 mL) was added dropwise to a stirred, cooled (0 °C) solution of *p*-toluenesulfonyl chloride (9.53 g, 50.0 mmol) in dry pyridine (30 mL). The mixture was allowed to warm to room temperature and stirred overnight. The mixture was poured into water, and the product was extracted into diethyl ether twice. The combined ethereal extracts were washed with 10% HCl twice and dried over anhydrous $MgSO_4$. The solvent was evaporated off, and the remaining crude product was purified by column chromatography (silica gel; hexane–ethyl acetate 10:1 and 5:1) to give a colorless liquid (8.88 g, 97.2%).

Scheme 2. Cationic Polymerization of 15 and 16

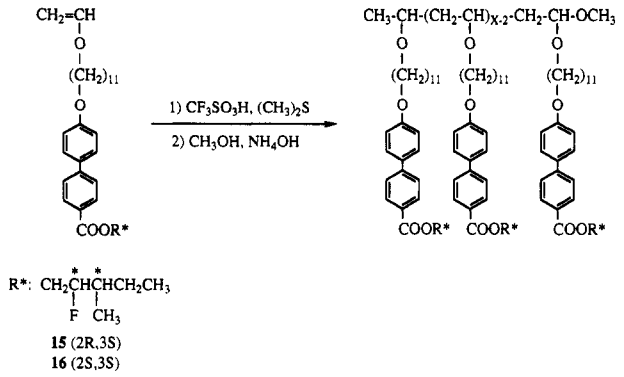

Purity: >99% (HPLC). ^{1}H-NMR ($CDCl_3$, TMS): δ 0.88 (t, J = 6.4 Hz, 3H, CH_3CH_2–), 0.90 (d, J = 6.0 Hz, 3H, –CH(CH_3)–), 1.08–1.31, 1.31–1.52 (m, 2H, CH_3CH_2–), 1.52–1.78 (m, 1H, –CH(CH_3)–), 2.45 (s, 3H, –PhCH_3), 4.15 (dd, J = 23.3 and 4.3 Hz, 2H, –CH_2OSO_2–), 4.51 (dq, J = 49.1 and 4.9 Hz, 1H, –CHF–), 7.37 (d, J = 8.0 Hz, 2ArH, ortho to –CH_3), 7.81 (d, J = 8.0 Hz, 2ArH, ortho to –SO_2–).

(2*R*,3*S*)-2-Fluoro-3-methylpentyl 4′-Hydroxybiphenyl-4-carboxylate (12). A mixture of 7 (7.80 g, 28.4 mmol), 11 (7.17 g, 28.4 mmol), TBAH (1.42 g), and dry DMSO (100 mL) was stirred at 80 °C under a nitrogen atmosphere for 20 h. The resulting clear yellow solution was poured into water. The product was extracted into diethyl ether twice, and the combined ethereal extracts were dried over anhydrous $MgSO_4$. The solvent was evaporated off, and the remaining crude product was purified by column chromatography (silica gel; hexane–ethyl acetate 4:1) to

Table 1. Cationic Polymerization of (2*R*,3*S*)-2-Fluoro-3-methylpentyl 4′-[[11-(Vinyloxy)undecanyl]oxy]biphenyl-4-carboxylate (15) and Characterization of the Resulting Polymers[a]

sample no.	$[M]_0/[I]_0$	polymer yield (%)	$M_n \times 10^{-3}$	M_w/M_n	DP	phase transitions (°C) and corresponding enthalpy changes (kcal/mru)[b] heating	cooling
1	2	31.7	1.8	1.07	3.4	K 45.3 (3.16) K 56.9 (0.34) S_C* 81.7 (0.07) S_A 90.6 (1.67) I S_X 36.2 (0.82) K 55.3 (1.99) S_C* 80.5 (0.07) S_A 89.8 (1.65) I	I 84.0 (–1.62) S_A 76.4 (–0.07) S_C* 29.8 (–0.40) S_X 18.2 (–0.93) K
2	3	54.8	2.2	1.11	4.3	K 47.0 (2.91) S_C* 85.7 (0.06) S_A 97.0 (1.62) I K 34.5 (0.59) S_X 38.6 (0.52) S_C* 85.3 (0.07) S_A 96.4 (1.64) I	I 90.3 (–1.58) S_A 81.0 (–0.06) S_C* 34.1(–0.45) S_X 20.7(–0.50) K
3	5	65.5	3.1	1.12	6.0	K 49.8 (2.35) S_C* 90.9 (0.03) S_A 106.5 (1.59) I K 38.8 (0.44) S_X 46.6 (0.58) S_C* 90.4 (0.06) S_A 105.9 (1.55) I	I 99.6 (–1.55) S_A 85.8 (–0.06) S_C* 41.6(–0.52) S_X 30.4(–0.31) K
4	8	80.1	4.0	1.13	7.7	K 54.0 (2.09) S_C* 94.3 (0.03) S_A 116.1 (1.57) I K 49.7 (0.32) S_X 54.1 (0.81) S_C* 94.2 (0.05) S_A 115.9 (1.57) I	I 109.5 (–1.53) S_A 90.0 (–0.06) S_C* 48.9(–0.92) S_X
5	12	76.2	4.3	1.17	8.4	K 54.8 (1.27) S_X 58.6 (0.78) S_C* 95.3 (0.04) S_A 118.0 (1.55) I S_X 57.9 (1.17) S_C* 95.3 (0.05) S_A 118.4 (1.51) I	I 111.9 (–1.49) S_A 90.9 (–0.06) S_C* 51.7 (–1.05) S_X
6	20	82.4	6.2	1.20	12.1	K 58.2 (0.72) S_X 64.8 (1.05) S_C* 97.6 (0.05) S_A 126.4 (1.45) I S_X 64.7 (1.15) S_C* 97.5 (0.04) S_A 126.2 (1.45) I	I 120.0 (–1.44) S_A 93.3 (–0.06) S_C* 59.0 (–1.04) S_X
7	30	83.3	8.1	1.19	15.7	K 59.9 (0.57) S_X 67.9 (1.10) S_C* 99.0 (0.04) S_A 130.5 (1.39) I S_X 67.9 (1.15) S_C* 99.0 (0.04) S_A 130.4 (1.40) I	I 123.4 (–1.39) S_A 94.0 (–0.06) S_C* 62.1 (–1.13) S_X

[a] Polymerization temperature, 0 °C; polymerization solvent, methylene chloride; $[M]_0$ = 0.224; $[Me_2S]_0/[I]_0$ = 10; polymerization time, 1 h. [b] Heating and cooling rates are 20 °C/min. Data on the first line are from the first heating and cooling scans. Data on the second line are from the second heating scan.

Table 2. Cationic Polymerization of (2*S*,3*S*)-2-Fluoro-3-methylpentyl 4′-[[11-(Vinyloxy)undecanyl]oxy]biphenyl-4-carboxylate (16) and Characterization of the Resulting Polymers[a]

sample no.	$[M]_0/[I]_0$	polymer yield (%)	$M_n \times 10^{-3}$	M_w/M_n	DP	phase transitions (°C) and corresponding enthalpy changes (kcal/mru)[b] heating	cooling
1	2	46.1	1.8	1.06	3.4	K 43.5 (2.60) K 55.6 (0.86) S_C* 78.0 (0.06) S_A 86.9 (1.64) I S_X 34.5 (0.65) K 55.0 (2.19) S_C* 78.2 (0.07) S_A 86.9 (1.64) I	I 80.8 (–1.60) S_A 73.9 (–0.06) S_C* 28.0 (–0.33) S_X 13.2 (–0.61) K
2	3	54.0	2.1	1.10	4.1	K 45.9 (2.81) S_C* 83.3 (0.06) S_A 93.3 (1.65) I K 30.5 (0.67) S_X 37.5 (0.60) S_C* 83.4 (0.06) S_A 93.4 (1.64) I	I 87.2 (–1.59) S_A 79.0 (–0.06) S_C* 32.9(–0.45) S_X 15.8(–0.31) K
3	5	70.1	2.8	1.16	5.5	K 48.9 (2.44) S_C* 89.4 (0.06) S_A 103.8 (1.70) I K 34.0 (0.36) S_X 45.4 (0.61) S_C* 89.5 (0.05) S_A 104.0 (1.62) I	I 96.9 (–1.57) S_A 84.7 (–0.05) S_C* 39.9(–0.57) S_X 25.2(–0.31) K
4	8	75.3	4.3	1.12	8.3	K 52.1 (1.98) S_C* 92.7 (0.04) S_A 114.1 (1.55) I K 49.2 (0.28) S_X 52.8 (0.76) S_C* 93.0 (0.04) S_A 114.3 (1.53) I	I 107.6 (–1.52) S_A 88.4 (–0.05) S_C* 47.5(–0.83) S_X
5	12	74.9	4.9	1.16	9.5	K 59.4 (1.88) S_C* 95.0 (0.04) S_A 119.7 (1.51) I S_X 59.2 (1.21) S_C* 95.1 (0.03) S_A 119.8 (1.50) I	I 112.7 (–1.48) S_A 90.2 (–0.05) S_C* 52.4(–0.95) S_X
6	20	76.9	6.5	1.13	12.6	K 57.6 (0.58) S_X 63.1 (1.13) S_C* 96.6 (0.03) S_A 126.4 (1.42) I S_X 64.3 (1.12) S_C* 97.9 (0.04) S_A 126.5 (1.36) I	I 119.6 (–1.40) S_A 92.0 (–0.05) S_C* 56.4 (–1.01) S_X
7	30	79.7	7.5	1.17	14.6	K 59.0 (0.43) S_X 66.3 (1.15) S_C* 97.4 (0.03) S_A 128.8 (1.37) I S_X 66.4 (1.17) S_C* 97.8 (0.04) S_A 129.3 (1.36) I	I 122.7 (–1.38) S_A 93.8 (–0.06) S_C* 59.8 (–1.09) S_X

[a] Polymerization temperature, 0 °C; polymerization solvent, methylene chloride; $[M]_0$ = 0.224; $[Me_2S]_0/[I]_0$ = 10; polymerization time, 1 h. [b] Heating and cooling rates are 20 °C/min. Data on the first line are from the first heating and cooling scans. Data on the second line are from the second heating scan.

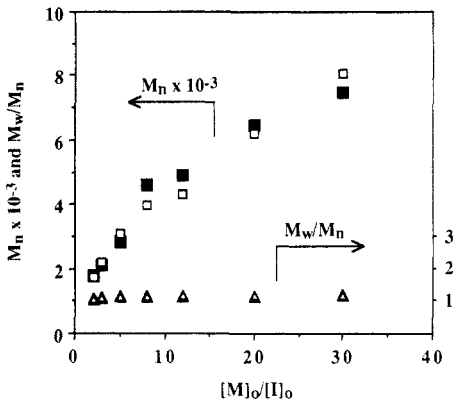

Figure 5. Dependence of the number-average molecular weight (M_n) and polydispersity (M_w/M_n) of poly(**15**) (open symbols) and poly(**16**) (closed symbols) determined by GPC on the $[M]_0/[I]_0$ ratio.

give a colorless solid which was recrystallized from hexane–ethyl acetate (40:1) to yield colorless crystals (5.77 g, 64.3%). Purity: >99% (HPLC). Mp: 95.4 °C (DSC, 20 °C/min). ^{1}H-NMR ($CDCl_3$, TMS): δ 0.96 (t, J = 7.0 Hz, 3H, CH_3CH_2–), 1.04 (d, J = 6.7 Hz, 3H, –CH(CH_3)–), 1.20–1.48, 1.48–1.67 (m, 2H, CH_3CH_2–), 1.67–2.07 (m, 1H, –CH(CH_3)–), 4.40–4.67, 4.79–4.91 (m, 3H, –CHFCH_2OCO–), 4.85 (b s, 1H, –PhOH), 6.96 (d, J = 8.7 Hz, 2ArH, ortho to –OH), 7.52 (d, J = 8.7 Hz, 2ArH, meta to –OH), 7.61 (d, J = 8.5 Hz, 2ArH, meta to –COO–), 8.11 (d, J = 8.5 Hz, 2ArH, ortho to –COO–).

(2*R*,3*S*)-2-Fluoro-3-methylpentyl 4′-[[11-(Vinyloxy)undecanyl]oxy]biphenyl-4-carboxylate (15). A mixture of **12** (4.50 g, 14.2 mmol), anhydrous K_2CO_3 (4.91 g, 35.5 mmol), and acetone (90 mL) was stirred at 60 °C under a nitrogen atmosphere for 2 h. To the resulting yellow solution was added a solution of **14** (3.94 g, 14.2 mmol) in dry DMSO (5.0 mL), and stirring was continued at 60 °C for 20 h. The mixture was poured into water, and the product was extracted into diethyl ether twice. The combined ethereal extracts were dried over anhydrous $MgSO_4$. The solvent was evaporated off, and the remaining crude product was purified by column chromatography twice (silica gel; hexane–ethyl acetate 30:1, 20:1, and 10:1) to yield a white solid (4.23 g, 58.1%). Purity: >99% (HPLC). The thermal transition temperatures are given in Table 3. ^{1}H-NMR ($CDCl_3$, TMS): δ 0.97 (t, J = 7.9 Hz, 3H, CH_3CH_2–), 1.04 (d, J = 7.0 Hz, 3H, –CH(CH_3)–), 1.31 (b s, 15H, CH_3CH_2–, CH_2=CHOCH$_2$CH$_2$(CH_2)$_7$–), 1.54–1.71 (m, 3H, CH_3CH_2–, CH_2=CHOCH$_2$CH_2–), 1.71–1.99 (m, 3H, –CH(CH_3)–, –CH_2CH$_2$OPh–), 3.67 (t, J = 6.5 Hz, 2H, CH_2=CHOCH_2–), 3.97 (dd, J = 6.9 and 1.9 Hz, 1H, CH_2=CHO– trans), 4.00 (t, J = 6.5 Hz, 2H, –CH_2OPh–), 4.17 (dd, J = 14.3 and 1.9 H z, 1H, CH_2=CHO– cis), 4.37–4.67, 4.78–4.88 (m, 3H, –CHFCH_2O–), 6.48 (dd, J = 14.3 and 6.9 Hz, 1H, CH_2=CHO–), 6.99 (d, J = 8.8 Hz, 2ArH, ortho to –(CH$_2$)$_{11}$O–), 7.57 (d, J = 8.8 Hz, 2ArH, meta to –(CH$_2$)$_{11}$O–), 7.64 (d, J = 8.5 Hz, 2ArH, meta to –COO–), 8.11 (d, J = 8.5 Hz, 2ArH, ortho to –COO–).

(2*S*,3*S*)-2-Fluoro-3-methylpentanoic Acid (8).[12a,13] Precooled (0 °C) dry pyridine (60 mL) was added dropwise to pyridinium poly(hydrogen fluoride) (HF, 70% by weight, 100 g) in a Teflon flask at 0 °C. L-Isoleucine (7.87 g, 60.0 mmol) was dissolved in this solution, and $NaNO_2$ (6.21 g, 90.0 mmol) was added in three portions over a period of 30 min at 0 °C with vigorous stirring. The reaction mixture was allowed to warm to room temperature, and stirring was continued for 5 h. The mixture was poured into water, and the product was extracted into diethyl ether three times using a Teflon separatory funnel. The combined ethereal extracts were dried over anhydrous $MgSO_4$. The solvent was evaporated off, and the remaining crude product was distilled under vacuum to yield a slightly yellow liquid (2.22 g, 27.6%). Bp: 78–80 °C (4 mmHg). ^{1}H-NMR (DMSO-d_6, TMS): δ 0.89 (t, J = 7.3 Hz, 3H, CH_3CH_2–), 0.97 (d, J = 7.0 Hz, 2H, –CH(CH_3)–), 1.06–1.32, 1.32–1.56 (m, 2H, CH_3CH_2–), 1.71–2.13 (m, 1H, –CH(CH_3)–), 4.81 (dd, J = 48.8 and 4.0 Hz, 1H, –CHF–).

(2*S*,3*S*)-2-Fluoro-3-methylpentanol (9). **9** was synthesized by the same procedure as the one used for the preparation of **6**. Starting from 4.50 g (33.5 mmol) of **8**, 2.52 g (67.0 mmol) of $LiAlH_4$, and 80 mL of dry THF, 2.40 g (59.6%) of **9** was obtained as a colorless liquid. ^{1}H-NMR ($CDCl_3$, TMS): δ 0.90 (d, J = 6.8 Hz, 3H, –CH(CH_3)–), 0.93 (t, J = 7.1 Hz, 3H, CH_3CH_2–), 1.09–1.37, 1.47–1.90 (m, 3H, CH_3CH_2CH(CH_3)–), 2.48 (s, 1H, –CH_2OH), 3.61–3.85 (m, 2H, –CH_2OH), 4.15–4.29, 4.40–4.53 (m 1H, –CHF–).

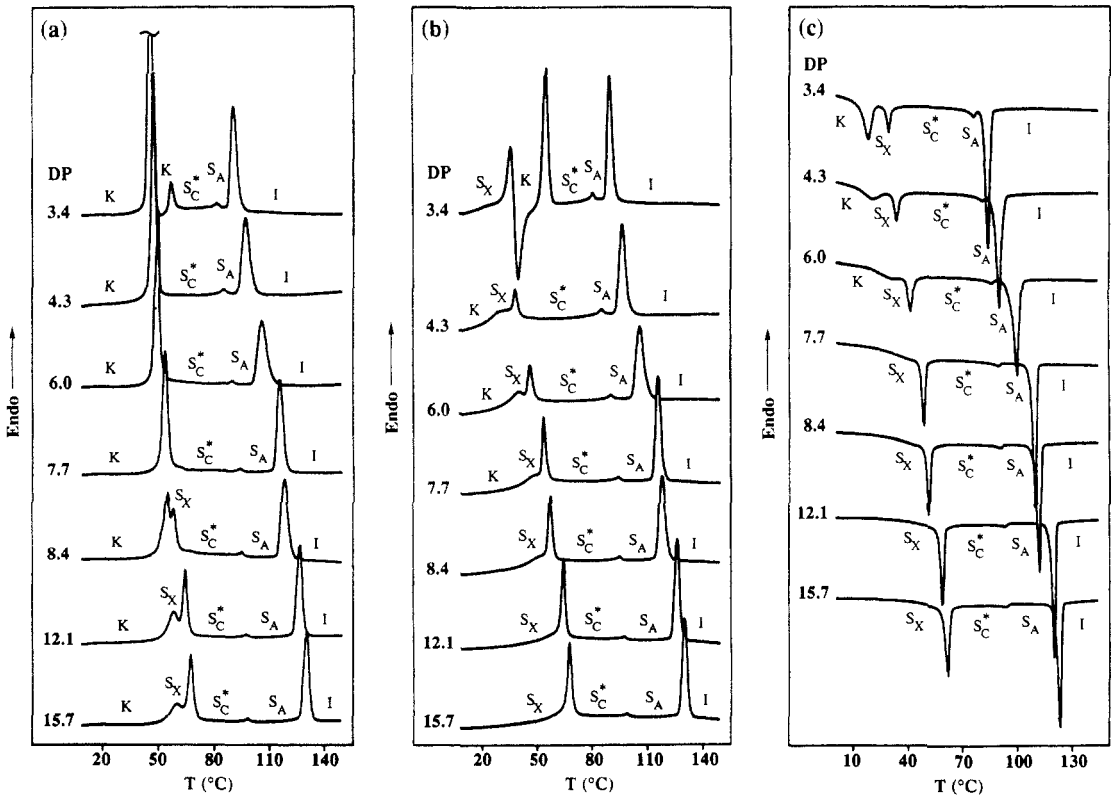

Figure 6. DSC thermograms (20 °C/min) of poly(**15**) with different DP: (a) first heating scans; (b) second heating scans; (c) first cooling scans.

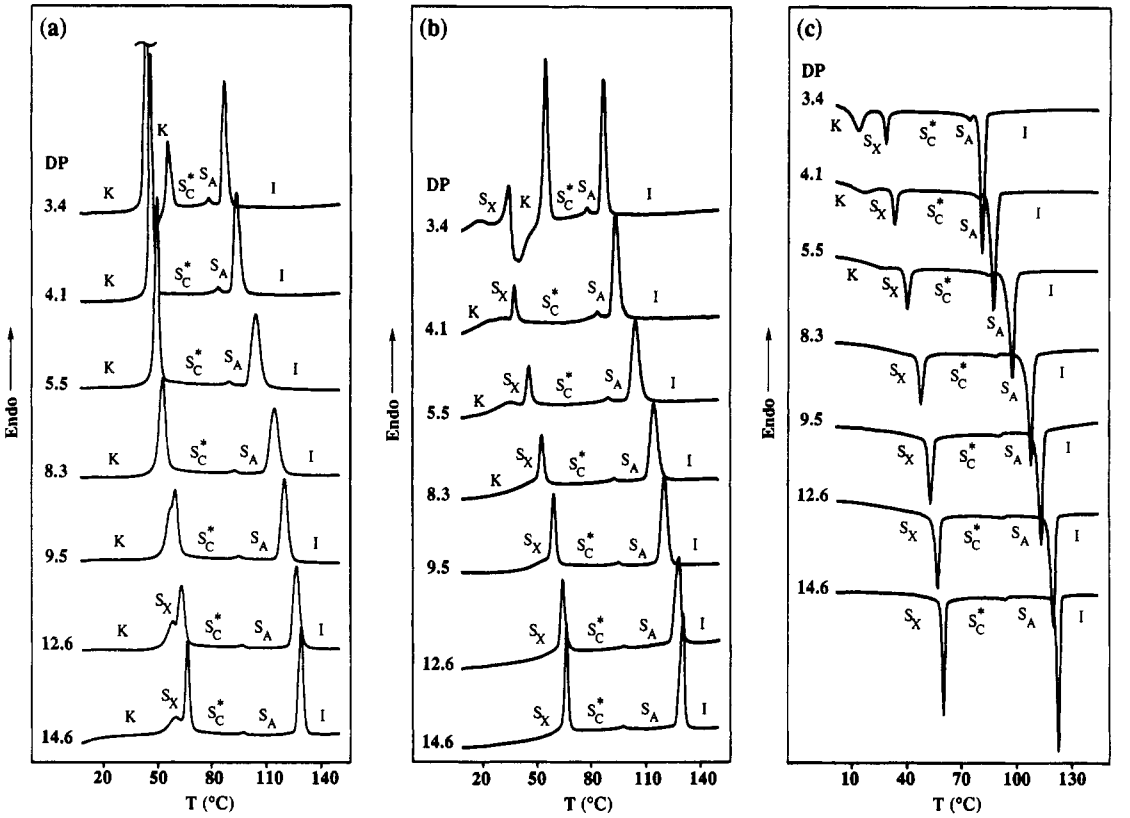

Figure 7. DSC thermograms (20 °C/min) of poly(16) with different DP: (a) first heating scans; (b) second heating scans; (c) first cooling scans.

(2*S*,3*S*)-2-Fluoro-3-methylpentyl Tosylate (10). 10 was synthesized by the same procedure as the one used for the preparation of 7. Starting from 1.80 g (15.0 mmol) of 7, 4.38 g (23.0 mmol) of *p*-toluenesulfonyl chloride, and 25 mL of dry pyridine, 3.88 g (94.3%) of 10 was obtained as a colorless liquid. Purity: 98.0% (HPLC). ^{1}H-NMR ($CDCl_3$, TMS): δ 0.86 (d, J = 7.3 Hz, 3H, $-CH(CH_3)-$), 0.88 (t, J = 7.8 Hz, 3H, CH_3CH_2-), 1.09–1.32, 1.42–1.62 (m, 2H, CH_3CH_2-), 1.62–1.89 (m, 1H, $-CH(CH_3)-$), 2.46 (s, 3H, $-PhCH_3$), 4.00–4.35, 4.47–4.59 (m, 3H, $-CHFCH_2O-$), 7.37 (d, J = 8.1 Hz, 2ArH, ortho to $-CH_3$), 7.81 (d, J = 8.1 Hz, 2ArH, ortho to $-SO_2-$).

(2*S*,3*S*)-2-Fluoro-3-methylpentyl 4′-Hydroxybiphenyl-4-carboxylate (13). 13 was synthesized by the same procedure as the one used for the preparation of 12. Starting from 3.00 g (10.9 mmol) of 10, 2.52 g (10.0 mmol) of 11, 0.50 g of TBAH, and 40 mL of dry DMSO, 2.27 g (71.7%) of 13 was obtained as colorless crystals. Purity: >99% (HPLC). Mp: 127.5 °C (DSC, 20 °C/min). ^{1}H-NMR ($CDCl_3$, TMS): δ 0.97 (t, J = 7.7 Hz, 3H, CH_3CH_2-), 1.00 (d, J = 7.1 Hz, 3H, $-CH(CH_3)-$), 1.19–1.45, 1.45–1.75 (m, 2H, CH_3CH_2-), 1.75–2.03 (m, 1H, $-CH(CH_3)-$), 4.33–4.90 (m, 3H, $-CHFCH_2O-$), 5.59 (b s, 1H, $-PhOH$), 6.95 (d, J = 8.6 Hz, 2ArH, ortho to $-OH$), 7.53 (d, J = 8.6 Hz, 2ArH, meta to $-OH$), 7.62 (d, J = 8.2 Hz, 2ArH, meta to $-COO-$), 8.11 (d, J = 8.2 Hz, 2ArH, ortho to $-COO-$).

(2*S*,3*S*)-2-Fluoro-3-methylpentyl 4′-[[11-(Vinyloxy)undecanyl]oxy]biphenyl-4-carboxylate (16). Monomer 16 was synthesized by the same procedure as the one used for the preparation of 15. Starting from 1.94 g (6.1 mmol) of 13, 1.66 g (6.0 mmol) of 14, 2.11 g (15.3 mmol) of anhydrous K_2CO_3, 2.5 mL of dry DMSO, and 50 mL of acetone, 1.28 g (40.8%) of 16 was obtained as a white solid. Purity: >99% (HPLC). The thermal transition temperatures are given in Table 3. ^{1}H-NMR ($CDCl_3$, TMS); δ 0.97 (t, J = 7.4 Hz, 3H, CH_3CH_2-), 1.00 (d, J = 6.9 Hz, 3H, $-CH(CH_3)-$), 1.31 (b s, 15H, CH_3CH_2-, $CH_2{=}CHOCH_2CH_2-(CH_2)_7-$), 1.56–1.72 (m, 3H CH_3CH_2-, $CH_2{=}CHOCH_2CH_2-$), 1.72–2.00 (m, 3H, $-CH(CH_3)-$, $-CH_2CH_2OPh-$), 3.67 (t, J = 6.6 Hz, 2H, $CH_2{=}CHOCH_2-$), 3.97 (dd, J = 6.9 and 1.9 Hz, 1H, $CH_2{=}CHO-$ trans), 4.01 (t, J = 6.5 Hz, 2H, $-CH_2OPh-$), 4.17 (dd, J = 14.1 and 1.9 Hz , 1H, $CH_2{=}CHO-$ cis), 4.29–4.79 (m, 3H, $-CHFCH_2O-$), 6.48 (dd, J = 14.1 and 6.9 Hz, 1H, $CH_2{=}CHO-$), 6.99 (d, J = 8.8 Hz, 2ArH, ortho to $-(CH_2)_{11}O-$), 7.57 (d, J = 8.8 Hz, 2ArH, meta to $-(CH_2)_{11}O-$), 7.63 (d, J = 8.5 Hz, 2ArH, ortho to $-COO-$), 8.11 (d, J = 8.5 Hz, 2ArH, meta to $-COO-$).

Cationic Polymerizations. Polymerizations were carried out in a three-necked round-bottom flask equipped with a Teflon stopcock and rubber septa under an argon atmosphere at 0 °C for 1 h. All glassware was dried overnight at 140 °C. The monomer was further dried under vacuum overnight in the polymerization flask. After the flask was filled with argon, freshly distilled dry CH_2Cl_2 was added via a syringe and the solution was cooled to 0 °C. $(CH_3)_2S$ and CF_3SO_3H were then added via a syringe. The monomer concentration was about 0.224 M, and the $(CH_3)_2S$ concentration was 10 times larger than that of CF_3SO_3H. The polymer molecular weight was controlled by the monomer/initiator ($[M]_0/[I]_0$) ratio. After quenching the polymerization with a mixture of NH_4OH and methanol (1:2), the reaction mixture was poured into methanol to give a white precipitate. The obtained polymer was purified by reprecipitation (chloroform solution, methanol) and dried under vacuum.

Results and Discussion

Determination of the Optical Purities of Monomers 15 and 16. The synthesis of the two diastereomeric monomers 15 and 16 is outlined in Scheme 1. The starting material, L-isoleucine (1), is one of the naturally occurring α-amino acids and has (2*S*,3*S*) configurations at the two chiral centers. In the course of transformation of L-isoleucine (1) into the fluorinated ester 5 and into the fluorinated acid 8, the amino group of L-isoleucine was first converted into a hydroxy group[12] (compound 2) and a fluorine atom[13] (compound 8), respectively, via a diazonium salt. These substitution reactions proceed with the retention of configuration at the C2 position because of the anchimeric assistance of the carboxylate group.[13] Compound 2 was further converted into triflate 4 which was substituted with a fluorine atom by using *n*-Bu_4NF.[12] As this substitution reaction proceeds with Walden inversion of the configuration at the C2 chiral center, compound 5 is expected to have (2*R*,3*S*) configurations, while compound 8 has (2*S*,3*S*) configurations. Compounds

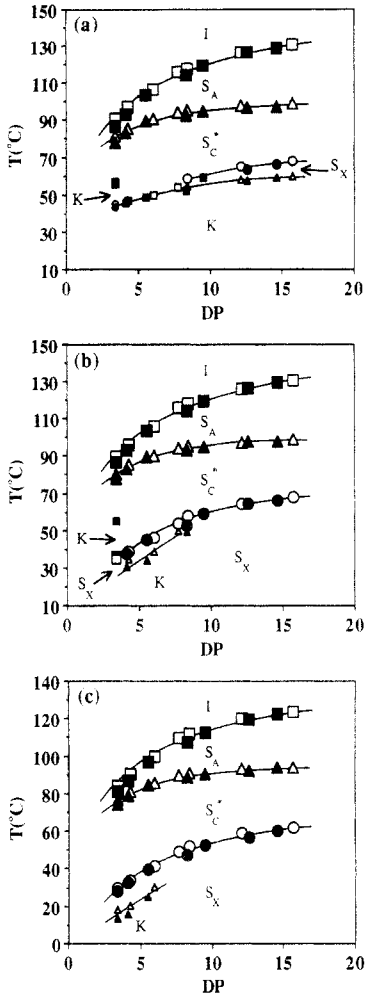

Figure 8. Dependence of phase transition temperatures on the degree of polymerization of poly(**15**) (open symbols) and poly(**16**) (closed symbols): (a) data from the first heating scans; (b) data from the second heating scans; (c) data from the first cooling scans.

5 and 8 are expected to be transformed into monomers **15** and **16** without any change of their configurations during the other steps of the synthesis.

The 200-MHz ^{1}H-NMR spectra of monomers **15** and **16** are shown in Figure 1. Figure 2 presents the 200-MHz ^{1}H-NMR spectra of the corresponding homopolymers, poly(**15**) (DP = 6.0) and poly(**16**) (DP = 5.5). These two figures clearly demonstrate that the signals due to the k and l protons (4.3–4.8 ppm) differ in their splitting patterns from each other between monomers **15** and **16** and between polymers poly(**15**) and poly(**16**). The peaks of poly(**15**) and poly(**16**) are similar to those of monomers **15** and **16**, respectively, although the polymers show broadened peaks.

In order to elucidate the assignment of these peaks ^{19}F-decoupled ^{1}H-NMR analysis was performed by using 300-MHz NMR spectroscopy. Figure 3 presents the ^{19}F-decoupled ^{1}H-NMR spectra (top) and the normal ^{1}H-NMR spectra (bottom) for the k and l protons of monomers **15** and **16** and polymers poly(**15**) and poly(**16**). In the ^{19}F-decoupled spectra the peaks show the AMNX pattern where A corresponds to the l proton, MN corresponds to the two k protons, and X corresponds to the fluorine atom. For **15** and poly(**15**), A (the l proton) can be assigned to the peaks at 4.71 ppm and MN (the two k protons) can be assigned to the peaks at 4.53 and 4.45 ppm, while for **16** and poly(**16**), A and M can be assigned to the peaks at 4.52–4.70 ppm and N can be assigned to the peaks at 4.44 ppm. Thus it is demonstrated that these two pairs of diastereomers have different structures and each diastereomer is expected to have high optical purity.

The optical purity arising from the C2 chiral center was successfully determined by a ^{19}F-NMR technique. The results are summarized in Figure 4. These spectra exhibit two clear clusters at −63.0 and −69.5 ppm, and it is obvious that the former corresponds to the 2*S* configuration and the latter corresponds to the 2*R* configuration. The optical purities calculated from the integration of these two clusters are 2*R* 96% (92% ee) for monomer **15** and 2*S* 98% (96% ee) for monomer **16**. The corresponding polymers poly(**15**) and poly(**16**) have the optical purity of 2*R* 98% (96% ee) and 2*S* 98% (96% ee), respectively, and it is demonstrated that no racemization has occurred at the C2 chiral center during the polymerization.

The optical purity arising from the C3 chiral center was not determined because the signal of the m proton was buried under the large signals due to the aliphatic spacer and the terminal alkyl chains. However, it is believed that the original optical purity of L-isoleucine is maintained at the C3 chiral center because of its chemical stability.

Homopolymerization of 15 and 16. The homopolymerizations of **15** and **16** are presented in Scheme 2. All polymerizations were carried out at 0 °C in CH_2Cl_2 by a living cationic polymerization technique using CF_3SO_3H/$(CH_3)_2S$ as an initiation system. Previous work in our laboratory[14] and others[16] has shown that the CF_3SO_3H-initiated polymerization of vinyl ethers in the presence of a Lewis base such as $(CH_3)_2S$ gives well-defined polymers with controlled molecular weights and narrow polydispersities. The polymerization mechanism is discussed in detail in previous publications.[11,14,15]

The characterization of poly(**15**) and poly(**16**) by gel permeation chromatography (GPC) and differential scanning calorimetry (DSC) is summarized in Tables 1 and 2, respectively. The low polymer yields are the result of the loss of polymer during purification. Relative number-average molecular weights of polymers determined by GPC exhibit a linear dependence on the initial concentration ratio of monomer to initiator ($[M]_0/[I]_0$) as shown in Figure 5. All polydispersities are less than 1.20. The $[M]_0/[I]_0$ ratio provides a very good control of the polymer molecular weight. All these features demonstrate the typical characteristics of the living polymerization mechanism. The absolute number-average molecular weights were difficult to determine by ^{1}H-NMR spectroscopy from the chain ends of the polymer owing to signal overlap.

The mesomorphic behaviors of poly(**15**) and poly(**16**) were investigated by DSC and thermal optical polarized microscopy. Figures 6 and 7 present the DSC thermograms of poly(**15**) and poly(**16**) with various degrees of polymerization (DP), respectively. The phase behaviors of the two diastereomeric homopolymers can be compared by superimposing the plots of the dependencies of their thermal transition temperatures as a function of DP (Figure 8). As observed from this figure the phase behavior of poly(**15**) is identical to that of poly(**16**). The DSC curves of first heating scan differ from those of second heating scan (Figures 6 and 7). However, second and subsequent heating scans exhibit identical DSC traces. First and subsequent cooling scans also exhibit identical DSC traces. On the first heating scan all polymers exhibit a crystalline phase. In polymers with DP ≤ 8.3 the crystalline phase melts into a S_C^* phase which is followed by S_C^*–S_A and S_A–I phase transitions. In polymers with DP ≥ 8.4 another higher order smectic phase (S_X) is observed between K and S_C^* phases. The nature of this S_X phase was not identified. On the second heating and cooling scans all

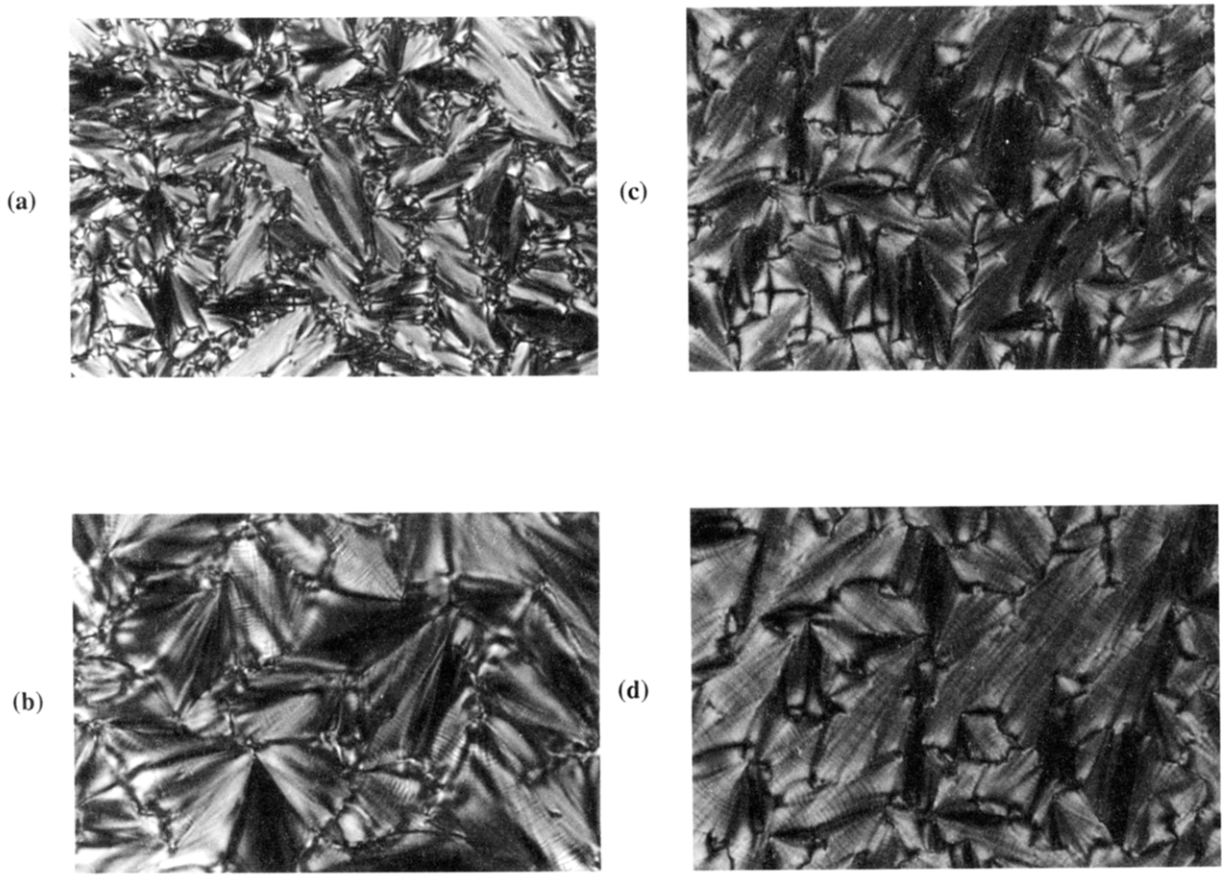

Figure 9. Representative optical polarized micrographs of: (a) the S_A mesophase displayed by poly(**15**) (DP = 7.7) upon cooling to 100 °C (100×); (b) the S_C* mesophase displayed by poly(**15**) (DP = 7.7) upon cooling to 69 °C (400×); (c) the S_C* mesophase displayed by poly(**16**) (DP = 8.3) upon cooling to 85 °C (400×); (d) the S_X mesophase displayed by poly(**16**) (DP = 8.3) upon cooling to 43 °C (400×). Magnifications have been reduced for publication.

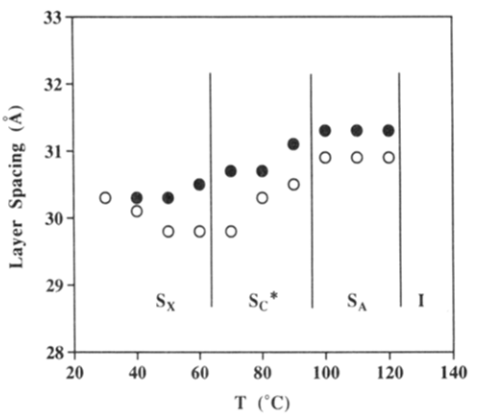

Figure 10. Temperature dependence of the layer spacing of poly(**15**) (DP = 11.8) (open symbols) and poly(**16**) (DP = 12.0) (closed symbols).

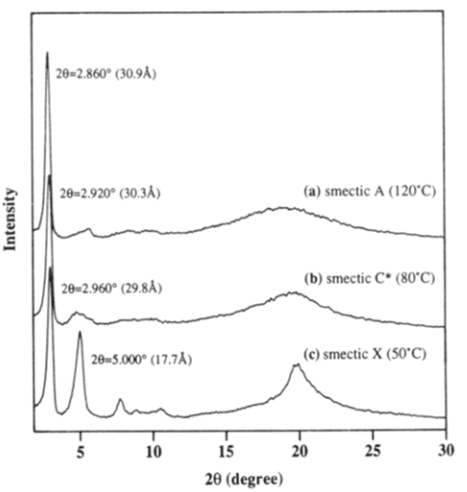

Figure 11. Representative X-ray diffraction diagrams of poly(**15**) (DP = 11.8).

polymers exhibit the S_X–S_C*–S_A–I phase sequence. The polymers with DP ≤ 6.0 have an additional crystalline phase. Especially polymers with DP = 3.4 crystallize on the second heating scan. This represents a classic example of the "polymer effect" which shows how the kinetically controlled crystallization process affects the stability of the thermodynamically controlled mesophase.[15b,17] The low molecular weight polymers exhibit a high rate of crystallization and, therefore, can crystallize on the second heating scan, while the higher molecular weight polymers have a much lower rate of crystallization and, subsequently, they do not crystallize on the second heating scan. Similar examples of this behavior are available both from our[11a,14a,15b,17] and from other laboratories.[18]

Representative optical polarized micrographs of the texture exhibited by the S_A and the S_C* phases of poly(**15**) (DP = 7.7) and the S_C* and the S_X phases of poly(**16**) (DP = 8.3) are presented in Figure 9.

In order to confirm the existence of the S_C* phase, X-ray diffraction measurements were carried out. Figure 10 presents the temperature dependence of the layer spacing obtained from poly(**15**) (DP = 11.8) and poly(**16**) (DP = 12.0). Representative X-ray diffraction diagrams of poly(**15**) (DP = 11.8) are shown in Figure 11. Measurements were performed on second heating scans, and the scanning rates were 2.5 °C/min, 10°/min, for poly(**15**) and 5.0 °C/min, 20°/min, for poly(**16**). With increasing the temper-

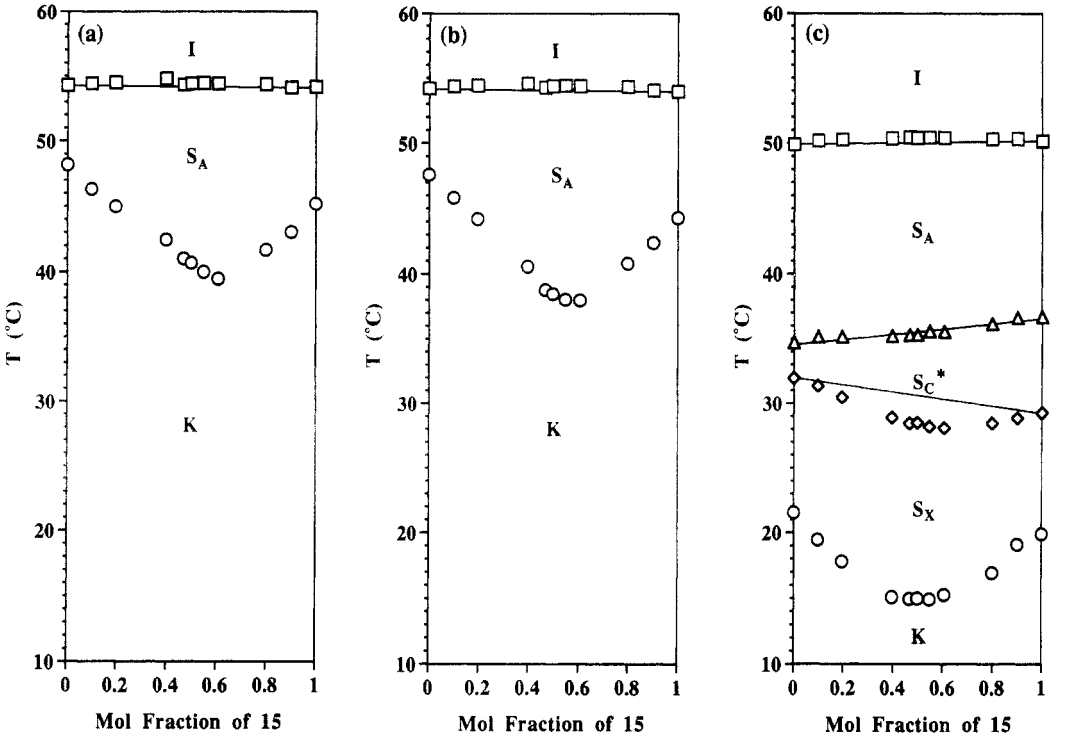

Figure 12. Dependence of phase transition temperatures on the composition of the binary mixtures of **15** with **16**: (a) data from the first heating scans; (b) data from the second heating scans; (c) data from the first cooling scans.

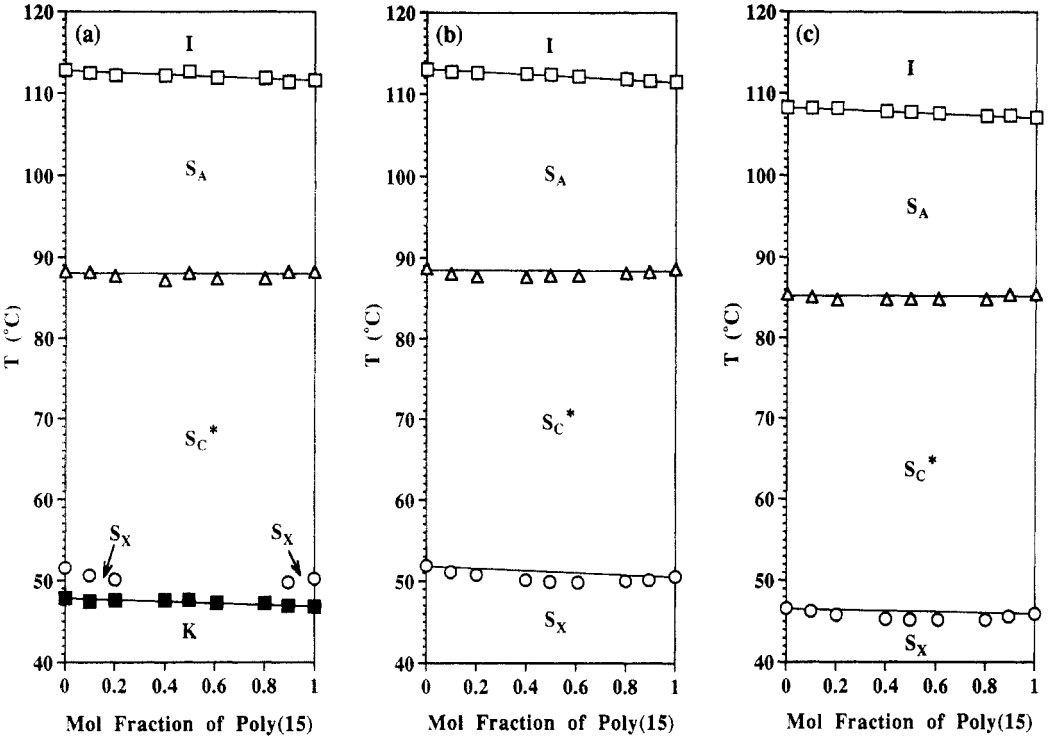

Figure 13. Dependence of phase transition temperatures on the composition of the binary mixtures of poly(**15**) (DP = 8.4) with poly(**16**) (DP = 9.5) (polymer mixtures I): (a) data from the first heating scans; (b) data from the second heating scans; (c) data from the first cooling scans.

ature the layer spacings of both polymers increase to reach constant values in between 90 and 100 °C which are in good agreement with the S_C*–S_A transition temperatures determined by the DSC analysis (*ca.* 97 °C). The layer spacings above 100 °C are about 31 Å, and this value is also in good agreement with the calculated side-chain length (32 Å) of both diastereomeric polymers. The difference of the layer spacing values between poly(**15**) and poly(**16**) shown in Figure 11 is probably due to the difference of the scanning rates. These results support the existence of the S_A phase and of the corresponding tilted phase (S_C* phase) in poly(**15**) and poly(**16**).

Miscibility Studies. Monomers **15** and monomer **16** were mixed in various compositions, and the phase behavior of their mixtures was investigated by DSC. Mixtures were prepared by dissolving the two monomers in CH_2Cl_2 followed by evaporation of the solvent under vacuum. Two sets of binary mixtures of poly(**15**) with poly(**16**) were also prepared, and their phase behaviors were investigated in the same manner. Polymer mixtures

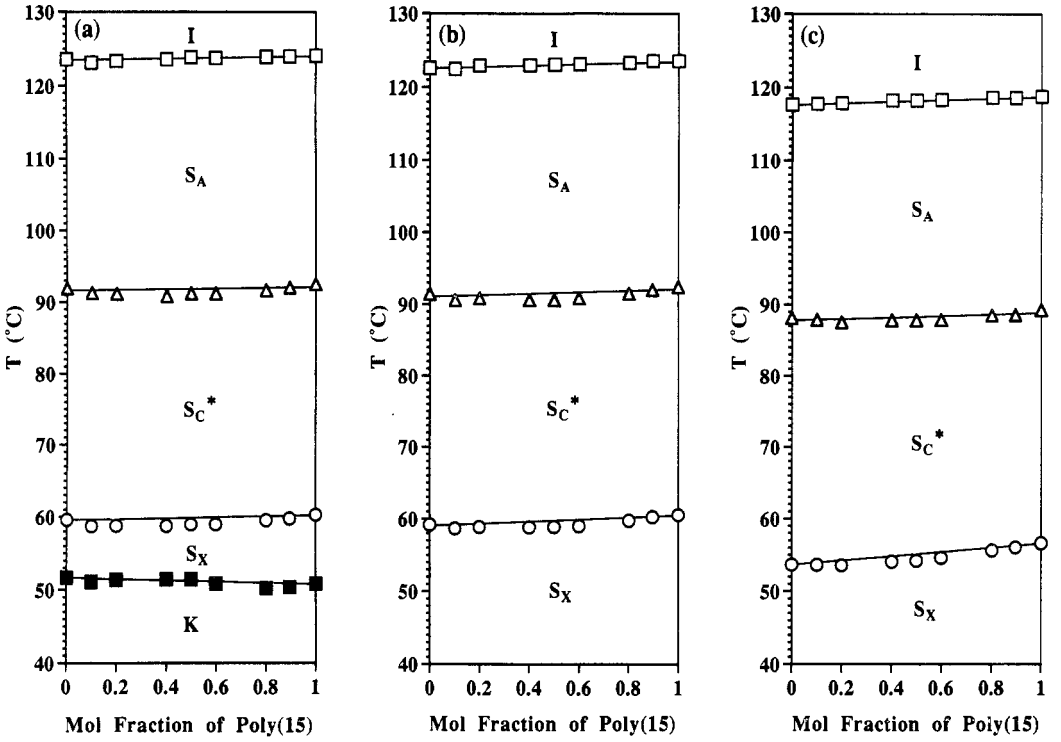

Figure 14. Dependence of phase transition temperatures on the composition of the binary mixtures of poly(**15**) (DP = 15.7) with poly(**16**) (DP = 14.6) (polymer mixtures II): (a) data from the first heating scans; (b) data from the second heating scans; (c) data from the first cooling scans.

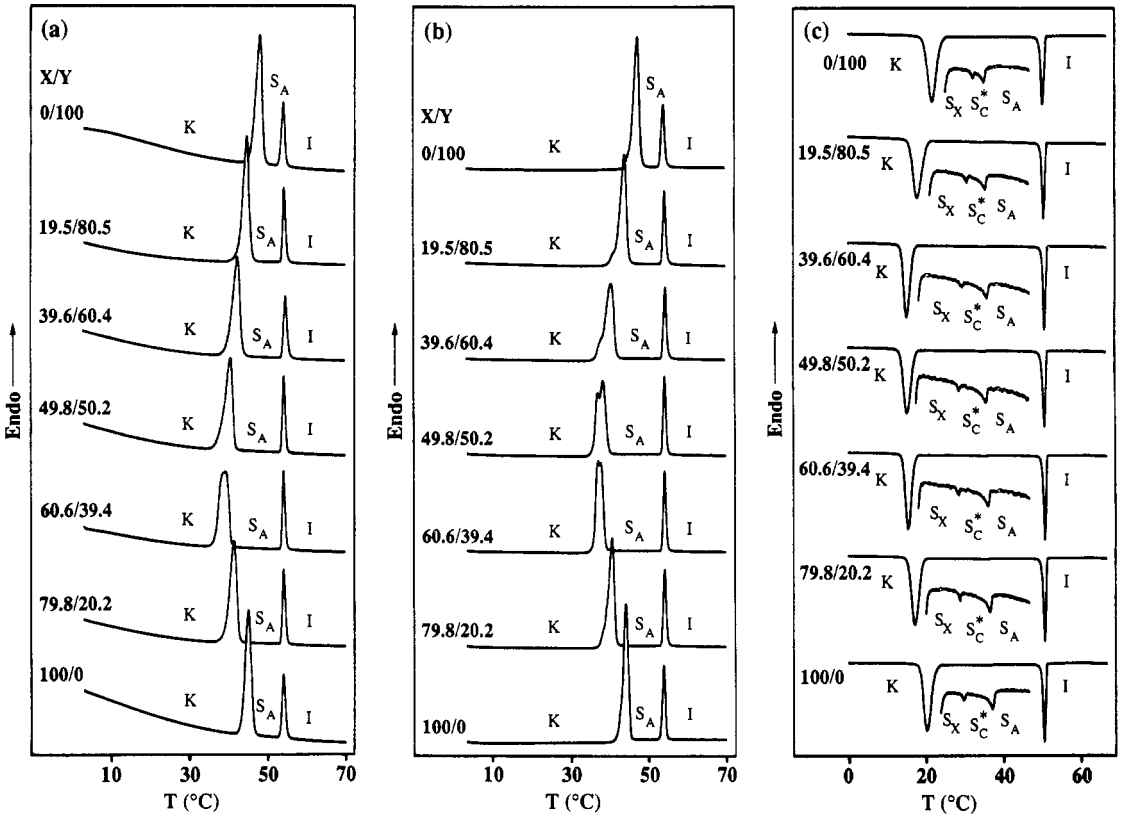

Figure 15. DSC thermograms (10 °C/min) of the binary mixtures of monomer 15 (X) with monomer 16 (Y): (a) first heating scans; (b) second heating scans; (c) first cooling scans.

I consist of poly(**15**) (DP = 8.4) and poly(**16**) (DP = 9.5), and polymer mixtures II consist of poly(**15**) (DP = 15.7) and poly(**16**) (DP = 14.6). The phase diagrams of the monomer mixtures are presented in Figure 12. The phase diagrams of the polymer mixtures I and II are presented in Figures 13 and 14, respectively. The thermal transition temperatures and the corresponding enthalpy changes are summarized in Tables 3–5. In Figure 15 the DSC thermograms of the monomer mixtures are presented.

The phase behavior of monomer **15** is very similar to that of monomer **16**. Both monomers display an enantiotropic S_A phase, monotropic S_C^* and S_X phases, and a crystalline phase. The transitions from the S_C^* phase into the S_X phase are very small on the DSC thermograms (Figure 15). Upon mixing the crystalline phase of the monomer system was suppressed and a eutectic compo-

Table 3. Characterization of the Binary Mixtures of Monomers 15 with 16

15/16 (mol/mol)	phase transitions (°C) and corresponding enthalpy changes (kcal/mol)[a]	
	heating	cooling
0/100	K 48.5 (5.84) S_A 54.3 (1.57) I K 47.6 (5.65) S_A 54.2 (1.56) I	I 49.9 (−1.56) S_A 34.7 (−0.02) S_C* 32.0 (−0.01) S_X 21.6 (−4.08) K
9.8/90.2	K 46.3 (5.81) S_A 54.4 (1.57) I K 45.9 (5.49) S_A 54.4 (1.57) I	I 50.2 (−1.58) S_A 35.2 (−0.03) S_C* 31.4 (−0.01) S_X 19.5 (−3.83) K
19.5/80.5	K 45.0 (5.68) S_A 54.5 (1.58) I K 44.2 (5.27) S_A 54.4 (1.57) I	I 50.3 (−1.58) S_A 35.2 (−0.04) S_C* 30.5 (−0.01) S_X 17.8 (−3.65) K
39.6/60.4	K 42.4 (5.37) S_A 54.8 (1.57) I K 40.6 (4.83) S_A 54.6 (1.57) I	I 50.4 (−1.57) S_A 35.2 (−0.03) S_C* 28.9 (−0.01) S_X 15.1 (−3.32) K
46.7/53.3	K 41.0 (5.28) S_A 54.3 (1.56) I K 37.2 (†[b]) K 38.8 (4.68) S_A 54.3 (1.57) I	I 50.5 (−1.57) S_A 35.3 (−0.04) S_C* 28.5 (−0.01) S_X 15.0 (−3.30) K
49.8/50.2	K 40.7 (5.22) S_A 54.4 (1.56) I K 37.1 (†[b]) K 38.5 (4.61) S_A 54.4 (1.56) I	I 50.4 (−1.58) S_A 35.3 (−0.03) S_C* 28.5 (−0.01) S_X 15.0 (−3.29) K
54.7/45.3	K 40.0 (5.06) S_A 54.4 (1.57) I K 37.1 (†[b]) K 38.0 (4.52) S_A 54.4 (1.56) I	I 50.4 (−1.57) S_A 35.6 (−0.04) S_C* 28.2 (−0.01) S_X 14.9 (−3.26) K
60.6/39.4	K 39.5 (5.01) S_A 54.4 (1.57) I K 37.2 (†[b]) K 38.0 (4.52) S_A 54.4 (1.58) I	I 50.4 (−1.57) S_A 35.6 (−0.03) S_C* 28.1 (−0.01) S_X 15.3 (−3.29) K
79.8/20.2	K 41.7 (5.16) S_A 54.3 (1.57) I K 40.8 (4.78) S_A 54.3 (1.58) I	I 50.3 (−1.58) S_A 36.2 (−0.03) S_C* 28.5 (−0.01) S_X 16.9 (−3.45) K
90.1/9.9	K 43.0 (5.25) S_A 54.1 (1.52) I K 42.4 (4.92) S_A 54.1 (1.54) I	I 50.3 (−1.54) S_A 36.6 (−0.04) S_C* 28.9 (−0.01) S_X 19.1 (−3.62) K
100/0	K 45.2 (5.49) S_A 54.1 (1.58) I K 44.3 (5.17) S_A 54.0 (1.57) I	I 50.1 (−1.56) S_A 36.7 (−0.03) S_C* 29.3 (−0.01) S_X 19.9 (−3.80) K

[a] Heating and cooling rates are 10 °C/min. Data on the first line are from the first heating and cooling scans. Data on the second line are from the second heating scan. [b] Overlapped peak.

Table 4. Characterization of the Binary Mixtures of Poly(15) with Poly(16) (Polymer Mixtures I)

DP		poly(15)/poly(16) (mol/mol)	phase transitions (°C) and corresponding enthalpy changes (kcal/mru)[a]	
poly(15)	poly(16)		heating	cooling
8.4	9.5	0/100	K 47.8 (0.71) S_X 51.6 (0.74) S_C* 88.2 (0.02) S_A 112.8 (1.43) I S_X 51.9 (1.16) S_C* 88.7 (0.04) S_A 113.0 (1.46) I	I 108.3 (−1.50) S_A 85.5 (−0.04) S_C* 46.6 (−0.95) S_X
8.4	9.5	9.9/90.1	K 47.4 (0.79) S_X 50.6 (0.68) S_C* 88.1 (0.03) S_A 112.5 (1.43) I S_X 51.1 (1.08) S_C* 88.1 (0.03) S_A 112.7 (1.47) I	I 108.3 (−1.51) S_A 85.1 (−0.03) S_C* 46.3 (−1.03) S_X
8.4	9.5	20.2/79.8	K 47.6 (0.86) S_X 50.1 (0.66) S_C* 87.7 (0.03) S_A 112.2 (1.43) I S_X 50.8 (1.18) S_C* 87.7 (0.03) S_A 112.6 (1.50) I	I 108.2 (−1.52) S_A 84.8 (−0.03) S_C* 45.8 (−1.00) S_X
8.4	9.5	40.0/60.0	K 47.6 (1.53) S_C* 87.1 (0.03) S_A 112.2 (1.46) I S_X 50.1 (1.14) S_C* 87.6 (0.04) S_A 112.5 (1.49) I	I 107.8 (−1.53) S_A 84.8 (−0.03) S_C* 45.3 (−1.02) S_X
8.4	9.5	49.7/50.3	K 47.6 (1.50) S_C* 88.0 (0.03) S_A 112.6 (1.47) I S_X 49.9 (1.16) S_C* 87.9 (0.04) S_A 112.4 (1.48) I	I 107.8 (−1.52) S_A 84.9 (−0.04) S_C* 45.2 (−1.00) S_X
8.4	9.5	60.9/39.1	K 47.3 (1.52) S_C* 87.3 (0.02) S_A 111.9 (1.46) I S_X 49.8 (1.12) S_C* 87.8 (0.04) S_A 112.2 (1.51) I	I 107.6 (−1.55) S_A 84.9 (−0.03) S_C* 45.2 (−1.05) S_X
8.4	9.5	80.1/19.9	K 47.2 (1.55) S_C* 87.4 (0.04) S_A 111.9 (1.46) I S_X 50.0 (1.16) S_C* 88.1 (0.04) S_A 111.8 (1.50) I	I 107.3 (−1.52) S_A 84.9 (−0.04) S_C* 45.2 (−0.99) S_X
8.4	9.5	89.5/10.5	K 46.9 (1.00) S_X 49.8 (0.58) S_C* 88.2 (0.03) S_A 111.4 (1.45) I S_X 50.2 (1.10) S_C* 88.3 (0.04) S_A 111.6 (1.48) I	I 107.3 (−1.50) S_A 85.4 (−0.04) S_C* 45.6 (−1.01) S_X
8.4	9.5	100/0	K 46.8 (0.95) S_X 50.2 (0.56) S_C* 88.2 (0.04) S_A 111.6 (1.48) I S_X 50.6 (1.19) S_C* 88.6 (0.04) S_A 111.5 (1.47) I	I 107.1 (−1.56) S_A 85.5 (−0.03) S_C* 46.0 (−0.97) S_X

[a] Heating and cooling rates are 10 °C/min. [b] Data on the first line are from the first heating and cooling scans. Data on the second line are from the second heating scan.

sition was observed. In the S_A, S_C*, and S_X mesophases the two diastereomeric structural units of the monomers are miscible and isomorphic across the full composition range. In the cooling scans the S_A–S_C* and the S_C*–S_X transition temperatures also showed negative deviations from the theoretical values which were calculated from the Schröder–van Laar equation for an ideal solution.[19,20] The deviations of the temperature in a 50/50 mixture are −0.4 °C for the S_A–S_C* transition and −2.1 °C for the S_C*–S_X transition. It seems that the transition involving a higher order phase shows a larger temperature deviation. On the contrary, the isotropization temperatures of the monomer mixtures are always higher (0.2–0.4 °C) than those of the pure monomers, and a slight upward curvature is observed in all scans.

The S_A–S_C* and S_C*–S_X transitions show a downward curvature in both of the polymer mixtures as well. The deviations of the temperature in a 50/50 mixture are around −1.0 °C in all cases. Polymer mixtures II have higher molecular weights than polymer mixtures I. However, it seems to be difficult to observe the molecular weight dependence in these transition temperature deviations. The isotropization temperatures of both polymer mixtures are insensitive to the optical purity, and no temperature deviations were observed within the experimental error.

Copolymerization of 15 with 16. Copolymerization of **15** with **16** was performed to cover the entire range of compositions. Attempts were made to synthesize poly(**15**-*co*-**16**) with DP = 16. Since the transition temperatures of polymers are strongly dependent on their molecular weights, it is essential to synthesize polymers having identical molecular weights in order to compare their transition temperatures. This can be achieved only by a living polymerization. The copolymerization results are

Table 5. Characterization of the Binary Mixtures of Poly(15) with Poly(16) (Polymer Mixtures II)

DP		poly(15)/poly(16)	phase transitions (°C) and corresponding enthalpy changes (kcal/mru)[a]	
poly(15)	poly(16)	(mol/mol)	heating	cooling
15.7	14.6	0/100	K 51.7 (0.45) S_X 59.6 (1.16) S_C* 92.0 (0.03) S_A 123.6 (1.44) I S_X 59.2 (1.11) S_C* 91.5 (0.04) S_A 122.6 (1.31) I	I 117.7 (−1.35) S_A 88.2 (−0.03) S_C* 53.7 (−1.00) S_X
15.7	14.6	10.1/89.9	K 51.1 (0.31) S_X 58.8 (1.07) S_C* 91.3 (0.04) S_A 123.2 (1.43) I S_X 58.7 (1.11) S_C* 90.6 (0.04) S_A 122.5 (1.32) I	I 117.8 (−1.33) S_A 87.9 (−0.04) S_C* 53.7 (−0.95) S_X
15.7	14.6	20.0/80.0	K 51.4 (0.33) S_X 58.9 (1.08) S_C* 91.2 (0.03) S_A 123.4 (1.46) I S_X 58.9 (1.13) S_C* 90.9 (0.04) S_A 123.0 (1.32) I	I 117.9 (−1.35) S_A 87.6 (−0.03) S_C* 53.6 (−0.95) S_X
15.7	14.6	40.1/59.9	K 51.5 (0.33) S_X 58.9 (1.08) S_C* 90.9 (0.03) S_A 123.6 (1.44) I S_X 58.8 (1.12) S_C* 90.6 (0.04) S_A 123.0 (1.33) I	I 118.3 (−1.36) S_A 87.9 (−0.03) S_C* 54.1 (−0.95) S_X
15.7	14.6	50.0/50.0	K 51.5 (0.31) S_X 59.1 (1.12) S_C* 91.3 (0.04) S_A 123.9 (1.43) I S_X 58.9 (1.15) S_C* 90.6 (0.03) S_A 123.1 (1.35) I	I 118.3 (−1.37) S_A 87.9 (−0.03) S_C* 54.3 (−0.98) S_X
15.7	14.6	59.9/40.1	K 50.9 (0.32) S_X 59.1 (1.07) S_C* 91.3 (0.03) S_A 123.8 (1.46) I S_X 59.0 (1.14) S_C* 90.9 (0.03) S_A 123.1 (1.36) I	I 118.5 (−1.36) S_A 87.9 (−0.03) S_C* 54.7 (−0.97) S_X
15.7	14.6	80.1/19.9	K 50.3 (0.43) S_X 59.7 (1.16) S_C* 91.8 (0.04) S_A 124.0 (1.52) I S_X 59.8 (1.13) S_C* 91.5 (0.04) S_A 123.3 (1.37) I	I 118.8 (−1.35) S_A 88.6 (−0.03) S_C* 55.7 (−0.93) S_X
15.7	14.6	89.6/10.4	K 50.4 (0.38) S_X 59.9 (1.10) S_C* 92.2 (0.04) S_A 124.0 (1.52) I S_X 60.3 (1.14) S_C* 92.1 (0.03) S_A 123.6 (1.34) I	I 118.7 (−1.36) S_A 88.6 (−0.03) S_C* 56.1 (−0.95) S_X
15.7	14.6	100/0	K 50.9 (0.38) S_X 60.4 (1.19) S_C* 92.7 (0.05) S_A 124.1 (1.66) I S_X 60.6 (1.15) S_C* 92.5 (0.04) S_A 123.6 (1.35) I	I 118.9 (−1.38) S_A 89.3 (−0.03) S_C* 56.7 (−0.97) S_X

[a] Heating and cooling rates are 10 °C/min. [b] Data on the first line are from the first heating and cooling scans. Data on the second line are from the second heating scan.

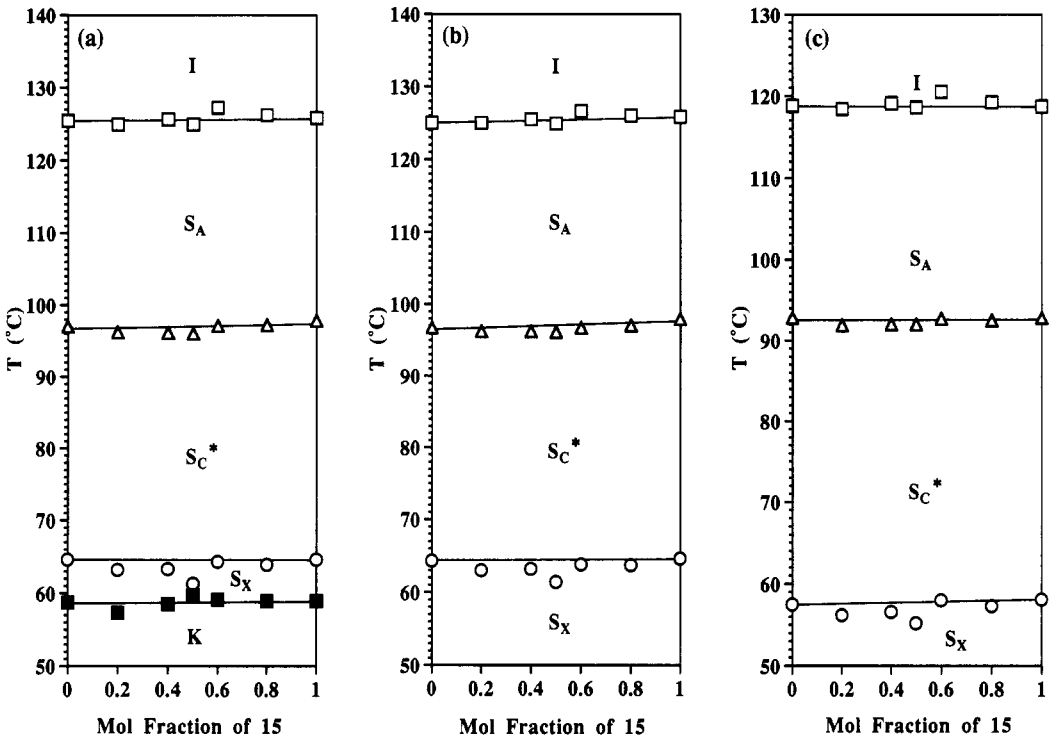

Figure 16. Dependence of phase transition temperatures on the composition of poly(15-*co*-16) (DP = 11.6–12.8): (a) data from the first heating scans; (b) data from the second heating scans; (c) data from the first cooling scans.

listed in Table 6. The yields reported in Table 6 are lower than quantitative due to polymer losses during the purification process. However, all conversions were quantitative and, therefore, the copolymer composition is identical to that of the monomer feed.[15b] The average degrees of polymerization determined by GPC are *ca.* 12.

The thermal transition temperatures determined by DSC are listed in Table 6 and plotted against copolymer composition in Figure 16. The copolymers poly(15-*co*-16) exhibit the same phase behavior as their parent homopolymers over the entire range of compositions. The S_A–S_C* transitions show clear negative deviations compared to the homopolymers in all scans. It appears that the S_C*–S_X transitions also exhibit negative deviations, although the fluctuation of data points can be seen due to the imperfect molecular weight control in the copolymerizations. The isotropization temperatures, however, remain insensitive to the copolymer compositions. As observed in Figure 8 the molecular weight dependence of the I–S_A transition temperature is larger than that of the

Table 6. Cationic Copolymerization of 15 with 16 and Characterization of the Resulting Polymers[a]

sample no.	[15]/[16] (mol/mol)	polymer yield (%)	$M_n \times 10^{-3}$	M_w/M_n	DP	phase transitions (°C) and corresponding enthalpy changes (kcal/mru)[b] heating	cooling
1	0/10	81.2	6.2	1.10	12.0	K 58.7 (0.59) S_X 64.6 (1.09) S_C* 97.0 (0.04) S_A 125.4 (1.45) I S_X 64.3 (1.15) S_C* 96.7 (0.03) S_A 125.0 (1.44) I	I 118.8 (−1.44) S_A 92.8 (−0.06) S_C* 57.5 (−1.07) S_X
2	2/8	80.0	6.0	1.12	11.6	K 57.3 (0.58) S_X 63.2 (1.09) S_C* 96.2 (0.06) S_A 124.9 (1.54) I S_X 63.0 (1.19) S_C* 96.2 (0.04) S_A 125.0 (1.42) I	I 118.4 (−1.44) S_A 91.9 (−0.05) S_C* 56.2 (−1.04) S_X
3	4/6	79.9	6.1	1.12	11.9	K 58.5 (0.62) S_X 63.3 (1.18) S_C* 96.1 (0.04) S_A 125.6 (1.47) I S_X 63.2 (1.17) S_C* 96.2 (0.04) S_A 125.5 (1.47) I	I 119.1 (−1.47) S_A 92.0 (−0.05) S_C* 56.6 (−1.03) S_X
4	5/5	69.3	6.2	1.10	12.0	K 59.7 (0.63) S_X 61.3 (1.12) S_C* 96.0 (0.04) S_A 124.9 (1.45) I S_X 61.4 (1.15) S_C* 96.1 (0.03) S_A 124.9 (1.45) I	I 118.6 (−1.43) S_A 92.0 (−0.06) S_C* 55.2 (−1.05) S_X
5	6/4	82.6	6.5	1.12	12.8	K 59.1 (0.64) S_X 64.3 (1.14) S_C* 97.1 (0.04) S_A 127.2 (1.43) I S_X 63.8 (1.20) S_C* 96.7 (0.04) S_A 126.6 (1.44) I	I 120.5 (−1.43) S_A 92.7 (−0.06) S_C* 58.0 (−1.05) S_X
6	8/2	82.4	6.0	1.12	11.7	K 58.9 (0.67) S_X 63.9 (1.10) S_C* 97.2 (0.04) S_A 126.2 (1.44) I S_X 63.7 (1.19) S_C* 97.0 (0.03) S_A 126.0 (1.44) I	I 119.2 (−1.45) S_A 92.5 (−0.07) S_C* 57.3 (−1.07) S_X
7	10/0	78.5	6.0	1.13	11.8	K 58.9 (0.70) S_X 64.6 (1.08) S_C* 97.8 (0.04) S_A 125.8 (1.44) I S_X 64.6 (1.20) S_C* 97.9 (0.05) S_A 125.8 (1.44) I	I 118.7 (−1.43) S_A 92.8 (−0.06) S_C* 58.1 (−1.00) S_X

[a] Polymerization temperature, 0 °C; polymerization solvent, methylene chloride; $[M]_0 = [15] + [16] = 0.224$; $[M]_0/[I]_0 = 16$; $[Me_2S]_0/[I]_0 = 10$; polymerization time, 1 h. [b] Heating and cooling rates are 20 °C/min. Data on the first line are from the first heating and cooling scans. Data on the second line are from the second heating scan.

S_A–S_C* and the S_C*–S_X transitions, resulting in the difficulty in the quantitative comparison of the I–S_A transition temperatures even among copolymers with slightly different molecular weights. It is likely that the optical purity dependence of the I–S_A transition is too small to be detected within the experimental error due to the molecular weight fluctuations of the copolymers, even if such a dependence exists. The S_A–S_C* transition is subject to very small molecular weight dependences at molecular weights higher than DP = 10, resulting in the clear composition dependence as shown in Figure 16 regardless of the molecular weight difference of the copolymers.

Chiral Molecular Recognition in the Mixtures of 15 with 16 and Poly(15) with Poly(16) and in Copolymers Poly(15-*co*-16). The phase behaviors of **15** and poly(**15**) are identical to those of **16** and poly(**16**), respectively, except that the monomers show slightly different transition temperatures from each other. The synthesis and the phase behavior of two low molar mass diastereomeric liquid crystals, 4′-(*n*-dodecanyloxy)-4-biphenylyl 2-fluoro-3-methylpentanoate (**17**), were reported by Arakawa et al.[12a] Their structures are related to those of monomers investigated in the present paper. The major difference between **17** and our monomers **15** and **16** is that **17** is based on a 4,4′-dihydroxybiphenyl mesogen whereas **15** and **16** are based on a 4′-hydroxybiphenyl-4-carboxylate mesogen. It should be noted that the phase behaviors of (2*R*,3*S*)-**17** and (2*S*,3*S*)-**17** are totally different; i.e., (2*R*,3*S*)-**17** exhibits S_C* and S_A phases, while (2*S*,3*S*)-**17** exhibits only a S_A phase, and this is in contrast to the results in our systems.

Miscibility studies and copolymerization studies have revealed that the two structural units derived from the diastereomeric monomers **15** and **16** are miscible and isomorphic[21] within all mesophases over the entire range of compositions. Generally speaking, when the two optically pure enantiomers are mixed and they form a solid solution, it is possible to classify the behavior of the solid solution into three categories.[1d] The first case is an ideal solution in which all the transition temperatures of the mixtures show a linear dependence on their compositions. This ideal behavior can be described by the Schröder–van Laar equation.[19,20] The second and third cases are nonideal solution behaviors, and their phase diagrams show a positive or negative deviation from the linear dependence with a maximum or minimum of the transition temperature, respectively. The positive deviation from the ideal behavior is caused by the interaction between the two chiral moieties of both enantiomers, and therefore we would like to refer to this deviation as chiral recognition. On the other hand, the negative deviation is only a manifestation of a nonideal solution behavior which is caused by the cancellation of dipole moments and the resulting stabilization of the racemic mixture. The two chiral moieties used in the present study are not enantiomeric but diastereomeric with each other. As mentioned above, however, the phase behaviors of **15** and poly(**15**) are almost identical to those of **16** and poly(**16**), respectively. For the transition temperatures of a binary mixture whose two components show almost identical transitions and enthalpy changes, the Schröder–van Laar equation always gives a linear dependence. Consequently, the upward curvature observed for the S_A–I transition temperatures in the monomer mixtures is indicative of positive deviations from the theoretical values, demonstrating the presence of chiral recognition between the two diastereomers in their S_A phase. In the polymer mixtures and the copolymers the S_A–I transitions show linear dependences on composition and, therefore, it seems that the chiral recognition present in the monomer mixtures is canceled or too small to be detected. On the other hand, the S_A–S_C* and the S_C*–S_X transition temperatures are always depressed and show downward curvatures in both monomer and polymer systems, indicating a nonideal solution behavior of the two diastereomeric structural units in the S_C* and the S_X mesophases. This result is not unexpected since physical properties of diastereomers are most frequently different.

Bahr et al.[4b,c] have investigated the influence of chirality on phase transitions in low molar mass ferroelectric liquid crystals containing a chlorine atom on their chiral centers. Their findings can be summarized as follows: (i) For transitions involving chiral smectic phases (e.g., S_C*–S_A*, S_G*–S_C*, S_G*–S_A*) dependence of the transition temperature on chirality was observed and these transition temperatures were always lower (0.8–1.0 °C) in racemates

than in pure optically active enantiomers, whereas for transitions between two nonchiral smectic phases (e.g., S_B–S_A, S_E–S_B) on dependence of the transition temperature on chirality was observed. (ii) In all compounds investigated the racemic mixtures showed 0.2–0.3 °C higher I–S_A transitions than those of the pure optically active enantiomers. They explained these two observations in terms of the stabilization effect of the spontaneous polarization and the steric packing effects of the chiral moieties, respectively. Our experimental results in the present study are in good agreement with these two findings.

The phase diagram of binary mixtures of enantiomeric liquid crystals as a function of enantiomeric excess was investigated for some antiferroelectric liquid crystals.[5] In all these studies, with decreasing enantiomeric excess the temperature range of the S_C* phase increase whereas the temperature range of S_{C_A}* (antiferroelectric S_C* phase) decreases. However, no attention was paid to the isotropization temperature, and no quantitative data on it are available. The chirality dependence of liquid crystalline mesophases was also investigated in low molar mass liquid crystals which exhibited twisted gray boundary phases, and 3–6 °C higher isotropization temperatures are reported in racemic modifications of some phenyl propiolate and tolan type liquid crystals.[6] The most remarkable example of the chiral molecular recognition was demonstrated by 1-methylheptyl terephthalylidenebis(aminocinnamates) in which a racemic mixture exhibits almost 30 °C higher isotropization temperature than the corresponding pure enantiomers.[7] The structural features encountered in these examples are that the substituent on the chiral center is a methyl group and that the chiral center is directly connected to the dipole moment (–COO–). The monomers employed in the present study have a less bulky fluorine atom on the chiral center, and this chiral center is located apart from the dipole moment mediated by a methylenic unit, allowing the free rotation of the terminal chiral group. It is possible to speculate that these two structural parameters are responsible for the very small effect of chiral recognition between the monomers **15** and **16** investigated in the present study. In addition, on going from **15** and **16** to poly(**15**), poly(**16**), and poly(**15**-*co*-**16**), the ability of chiral recognition between the same two diastereomers is reduced even more. This is most probably due to the restrictions imposed by the polymer backbone and tacticity in the case of homopolymers and the polymer backbone, sequence distribution, and tacticity in the case of copolymers.

Acknowledgment. Financial support by the Office of Naval Research and Asahi Chemical Industry Co., Ltd., Japan, is gratefully acknowledged. We also thank Professor S. Z. D. Cheng of University of Akron for the X-ray measurements.

References and Notes

(1) (a) Arnett, E. M.; Harvey, N. G.; Rose, P. L. *Acc. Chem. Res.* **1989**, *22*, 131. (b) Rose, P. L.; Harvey, N. G.; Arnett, E. M. In *Advances in Physical Organic Chemistry, Vol. 28*; Bethell, D., Ed.; Academic Press: New York, 1993; p 45. (c) Pirkle, W. H.; Pochapsky, T. C. *Chem. Rev.* **1989**, *89*, 347. (d) Jacques, J.; Collet, A.; Wilen, S. H. *Enantiomers, Racemates and Resolutions*; Krieger Publishing Co.: Malabar, FL, 1991.

(2) (a) Arnett, E. M.; Thompson, O. *J. Am. Chem. Soc.* **1981**, *103*, 968. (b) Harvey, N. G.; Rose, P. L.; Mirajovsky, D.; Arnett, E. M. *J. Am. Chem. Soc.* **1990**, *112*, 3547.

(3) Arnett, E. M.; Gold, J. M. *J. Am. Chem. Soc.* **1982**, *104*, 636.

(4) (a) Leclercq, M.; Billard, J.; Jacques, J. *Mol. Cryst. Liq. Cryst.* **1969**, *8*, 367. (b) Bahr, CH.; Heppke, G.; Sabaschus, B. *Ferroelectrics* **1988**, *84*, 103. (c) Bahr, CH.; Heppke, G.; Sabaschus, B. *Liq. Cryst.* **1991**, *9*, 31.

(5) (a) Yamada, Y.; Mori, K.; Yamamoto, N.; Hayashi, H.; Nakamura, K.; Yamawaki, M.; Orihara, H.; Ishibashi, Y. *Jpn. J. Appl. Phys.* **1989**, *28*, L1606. (b) Takezoe, H.; Lee, J.; Chandani, A. D. L.; Gorecka, E.; Ouchi, Y.; Fukuda, A.; Terashima, K.; Furukawa, K. *Ferroelectrics* **1991**, *114*, 187. (c) Takezoe, H.; Fukuda, A.; Ikeda, A.; Takanishi, Y.; Umemoto, T.; Watanabe, J.; Iwane, H.; Hara, M.; Itoh, K. *Ferroelectrics* **1991**, *122*, 167. (d) Goodby, J. W.; Chin, E. *Liq. Cryst.* **1988**, *3*, 1245. (e) Goodby, J. W.; Patel, J. S.; Chin, E. *J. Mater. Chem.* **1992**, *2*, 197. (f) Heppke, G.; Lötzsch, D.; Demus, D.; Diele, S.; Jahn, K.; Zaschke, H. *Mol. Cryst. Liq. Cryst.* **1991**, *208*, 9.

(6) (a) Goodby, J. W.; Waugh, M. A.; Stein, S. M.; Chin, E.; Pindak, R.; Patel, J. S. *J. Am. Chem. Soc.* **1989**, *111*, 8119. (b) Slaney, A. J.; Goodby, J. W. *Liq. Cryst.* **1991**, *9*, 849. (c) Goodby, J. W.; Nishiyama, I.; Slaney, A. J.; Booth, C. J.; Toyne, K. J. *Liq. Cryst.* **1993**, *14*, 37. (d) Nguyen, H. T.; Twieg, R. J.; Nabor, M. F.; Isaert, N.; Destrade, C. *Ferroelectrics* **1991**, *121*, 187.

(7) (a) Levelut, A. M.; Germain, C.; Keller, P.; Liebert, L.; Billard, J. *J. Phys. (Paris)* **1983**, *44*, 623. (b) Keller, P. *Mol. Cryst. Liq. Cryst., Lett.* **1984**, *102*, 295. (c) Billard, J.; Dahlgren, A.; Flatischler, K.; Lagerwall, S. T.; Otterholm, B. *J. Phys. (Paris)* **1985**, *46*, 1241. (d) Heppke, G.; Kleineberg, P.; Lötzsch, D. *Liq. Cryst.* **1993**, *14*, 67.

(8) (a) Harvey, N.; Rose, P.; Porter, N. A.; Huff, J. B.; Arnett, E. M. *J. Am. Chem. Soc.* **1988**, *110*, 4395. (b) Heath, J. G.; Arnett, E. M. *J. Am. Chem. Soc.* **1992**, *114*, 4500.

(9) (a) Burdon, J.; Farazmand, I.; Stacey, M.; Tatlow, J. C. *J. Chem. Soc.* **1957**, 2574. (b) Stang, P. J.; Hanack, M.; Subramanian, L. R. *Synthesis* **1982**, 85. (c) Beard, C. D.; Baum, K.; Grakauskas, V. *J. Org. Chem.* **1973**, *38*, 3673.

(10) Dungan, C. H.; Van Wazer, J. R. *Compilation of Reported ^{19}F NMR Chemical Shifts*; Wiley-Interscience: New York, 1970.

(11) (a) Percec, V.; Zheng, Q.; Lee, M. *J. Mater. Chem.* **1991**, *1*, 611. (b) Percec, V.; Zheng, Q.; Lee, M. *J. Mater. Chem.* **1991**, *1*, 1015. (c) Percec, V.; Zheng, Q. *J. Mater. Chem.* **1992**, *2*, 475. (d) Percec, V.; Zheng, Q. *J. Mater. Chem.* **1992**, *2*, 1041.

(12) (a) Arakawa, S.; Nito, K.; Seto, J. *Mol. Cryst. Liq. Cryst.* **1991**, *204*, 15. (b) Chan, L. K. M.; Gray, G. W.; Lacey, D.; Scrowston, R. M.; Shenouda, I. G. *Mol. Cryst. Liq. Cryst.* **1989**, *172*, 125.

(13) (a) Olah, G. A.; Welch, J. *Synthesis* **1974**, 652. (b) Olah, G. A.; Welch, J. T.; Vankar, Y. D.; Nojima, M.; Kerekes, I.; Olah, J. A. *J. Org. Chem.* **1979**, *44*, 3872. (c) Keck, R.; Rétey, J. *Helv. Chim. Acta* **1980**, *63*, 769. (d) Olah, G. A.; Prakash, G. K.; Chao, Y. L. *Helv. Chim. Acta* **1981**, *64*, 2528. (e) Faustint, F.; Munari, S. D.; Panzeri, A.; Villa, V.; Gandolfi, C. A. *Tetrahedron Lett.* **1981**, *22*, 4533. (f) Barber, J.; Keck, R.; Rétey, J. *Tetrahedron Lett.* **1982**, *23*, 1549.

(14) (a) Percec, V.; Lee, M.; Jonsson, H. *J. Polym. Sci., Polym. Chem. Ed.* **1991**, *29*, 327. (b) Percec, V.; Lee, M. *Macromolecules* **1991**, *24*, 1017.

(15) (a) Percec, V.; Lee, M.; Rinaldi, P.; Litman, V. E. *J. Polym. Sci., Polym. Chem. Ed.* **1992**, *30*, 1213. (b) For a brief review on the molecular engineering of side-chain LCP by living cationic polymerization, see: Percec, V.; Tomazos, D. *Adv. Mater.* **1992**, *4*, 548.

(16) (a) Cho, C. G.; Feit, B. A.; Webster, O. W. *Macromolecules* **1990**, *23*, 1918. (b) Cho, C. G.; Feit, B. A.; Webster, O. W. *Macromolecules* **1992**, *25*, 2081. (c) Lin, C. H.; Matyjaszewsky, K. *Polym. Prepr. (Am. Chem. Soc., Div. Polym. Chem.)* **1990**, *31*, 599.

(17) (a) Percec, V.; Tomazos, D.; Pugh, C. *Macromolecules* **1989**, *22*, 3259. (b) Rodriguez-Parada, J. M.; Percec, V. *J. Polym. Sci., Polym. Chem. Ed.* **1986**, *24*, 1363. (c) Rodenhouse, R.; Percec, V.; Feiring, A. E. *J. Polym. Sci., Polym. Lett. Ed.* **1990**, *28*, 345. (d) Percec, V.; Lee, M. *Macromolecules* **1991**, *24*, 2780. (e) Percec, V.; Lee, M. *Polymer* **1991**, *32*, 2862. (f) Percec, V.; Lee, M. *Polym. Bull.* **1991**, *25*, 123. (g) Jonsson, H.; Percec, V.; Hult, A. *Polym. Bull.* **1991**, *25*, 115. (h) Percec, V.; Gomes, A. D. S.; Lee, M. *J. Polym. Sci., Polym. Chem. Ed.* **1991**, *29*, 1615. (i) Percec, V.; Wang, C. S. *Polym. Bull.* **1991**, *26*, 15.

(18) (a) Sagane, T.; Lenz, R. W. *Polym. J.* **1988**, *20*, 923. (b) Sagane, T.; Lenz, R. W. *Polymer* **1989**, *30*, 2269. (c) Sagane, T.; Lenz, R. W. *Macromolecules* **1989**, *22*, 3763.

(19) (a) Van Hecke, G. R. *J. Phys. Chem.* **1979**, *83*, 2344. (b) Achard, M. F.; Mauzac, M.; Richard, H.; Sigaud, G.; Hardouin, F. *Eur. Polym. J.* **1989**, *25*, 593.

(20) (a) Percec, V.; Lee, M. *J. Mater. Chem.* **1991**, *1*, 1007. (b) Percec, V.; Lee, M.; Zheng, Q. *Liq. Cryst.* **1992**, *12*, 715. (c) Percec, V.; Johansson, G. *J. Mater. Chem.* **1993**, *3*, 83.

(21) Percec, V.; Tsuda, Y. *Polymer* **1991**, *32*, 661.